AD_____

Award Number: W81XWH-06-1-0015

TITLE: Stathmin: A “Relay Protein” in the Development of Prostate Cancer and a Potential Target for Anti-cancer Therapy

PRINCIPAL INVESTIGATOR: Ritwik Ghosh

CONTRACTING ORGANIZATION: Vanderbilt University Medical Center
Nashville, TN 37232

REPORT DATE: November 2007

TYPE OF REPORT: Annual Summary

PREPARED FOR: U.S. Army Medical Research and Materiel Command
Fort Detrick, Maryland 21702-5012

DISTRIBUTION STATEMENT: Approved for Public Release;
Distribution Unlimited

REPORT DOCUMENTATION PAGE

Form Approved
OMB No. 0704-0188

1. REPORT DATE *(DD-MM-YYYY)*	**2. REPORT TYPE**	**3. DATES COVERED** *(From - To)*
01-11-2007	Annual Summary	15 OCT 2006 - 14 OCT 2007

4. TITLE AND SUBTITLE

Stathmin: A "Relay Protein" in the Development of Prostate Cancer and a Potential Target for Anti-cancer Therapy

5a. CONTRACT NUMBER

5b. GRANT NUMBER
W81XWH-06-1-0015

5c. PROGRAM ELEMENT NUMBER

6. AUTHOR(S)
Ritwik Ghosh

E-Mail: ritwik.ghosh@vanderbilt.edu

5d. PROJECT NUMBER

5e. TASK NUMBER

5f. WORK UNIT NUMBER

7. PERFORMING ORGANIZATION NAME(S) AND ADDRESS(ES)

Vanderbilt University Medical Center
Nashville, TN 37232

8. PERFORMING ORGANIZATION REPORT NUMBER

9. SPONSORING / MONITORING AGENCY NAME(S) AND ADDRESS(ES)
U.S. Army Medical Research and Materiel Command
Fort Detrick, Maryland 21702-5012

10. SPONSOR/MONITOR'S ACRONYM(S)

11. SPONSOR/MONITOR'S REPORT NUMBER(S)

12. DISTRIBUTION / AVAILABILITY STATEMENT
Approved for Public Release; Distribution Unlimited

13. SUPPLEMENTARY NOTES

14. ABSTRACT
The long term goal of this work is to determine whether stathmin can be targeted as an effective therapy in the clinic against prostate cancer (PCa). The purpose of this work is to i)correlate stathmin overexpression withprogression of PCa, ii) determine the signaling pathways activated through selective phosphorylation of stathmin and whether inactivation of these pathways promotes sensitization to treatment with Taxotere or Erbitux iii)examine the effects of stathmin expression on tumor development and the outcomes of Taxotere, Erbitux on blocking tumorigenesis in tissue recombination and and transgenic mouse models. We have identified that stathmin modulates TGFβ signaling in inducing epithelial-to-mesenchymal transformation of PCa cells. We have also established for the first time that p38MAPK acts downstream of stathmin in this pathway. Loss of stathmin results in the sequestering of phosphorylated Smad in the cellular cytoplasm. In its place, the Smad-independent MAPKpathway is activated as seen by p38 phosphorylation and the appearance of spindle-shaped cells. Thus we have identified stathmin as a major regulator of epithelial cell homeostasis.

15. SUBJECT TERMS
Stathmin, Tumorigenesis, Prostate Cancer, Prostatic Intraepithelial Neoplasia (PIN), Adenocarcinoma, Transgenic Mouse Model, Tissue Recombination, Taxotere, Erbitux.

16. SECURITY CLASSIFICATION OF:			**17. LIMITATION OF ABSTRACT**	**18. NUMBER OF PAGES**	**19a. NAME OF RESPONSIBLE PERSON**
a. REPORT	**b. ABSTRACT**	**c. THIS PAGE**			USAMRMC
U	U	U	UU	34	**19b. TELEPHONE NUMBER** *(include area code)*

Table of Contents

Annual Report
PCRP Predoctoral Traineeship Award
W81XWH-06-1-015
Stathmin: A "Relay Protein" in the Development of Prostate Cancer and a Potential Target for Anti-cancer Therapy
P.I. Ritwik Ghosh, PhD

Introduction

The **long term goal** of this project is to determine whether stathmin can be targeted as an effective therapy in the clinic against prostate cancer (PCa). The **central hypothesis** of this proposal is that *overexpression of stathmin promotes PCa development and blocking stathmin expression sensitizes PCa cells to anti-cancer therapies such as taxotere and erbitux.* The **purpose** of this work is to i) correlate stathmin overexpression with progression of PCa, ii) determine the signaling pathways activated through selective phosphorylation of stathmin and whether inactivation of these pathways promotes sensitization to treatment with Taxotere or Erbitux and iii) examine the effects of stathmin expression on tumor development and the outcomes Taxotere and Erbitux on blocking tumorigenesis in tissue recombination and transgenic mouse models. The **rationale** is to develop combinatorial treatment strategies for better clinical management of PCa patients. Targeting stathmin in PCa can potentially sensitize patients to treatment with Taxotere or Erbitux. Since the agents selected have already been used in the clinic, successful outcomes in the animal models can result in rapid clinical trials.

Statement of Work
PCRP Predoctoral Traineeship Award
W81XWH-06-1-015
Stathmin: A "Relay Protein" in the Development of Prostate Cancer and a Potential Target for Anti-cancer Therapy
P.I. Ritwik Ghosh, PhD

Task 1

Investigate how the levels of stathmin expression regulates tumorigenesis in prostate cancer cells

a) Study stathmin expression by immunohistochemistry in tissue arrays containing low grade and high grade human prostate samples from 111 patients to analyze and semi-quantify the levels of stathmin expression as they increase with cancer grade. The levels of stathmin expression to be compared to that in benign prostatic hyperplasia (BPH).

   Status: Stathmin expression has been studied in tissue arrays arranged according to Gleason Pattern. The initial immunohistochemistry on a tissue array containing 111 patient samples exhibited background staining and hence was not fit for any statistical analyses. New tissue arrays were procured from The Prostate Cancer Center at Vancouver General Hospital, University of British Columbia, British Columbia, Canada. A total of 200 cores from 50 BPH and PCa patients were arrayed in a sequential pattern from Gleason Pattern 3 to 5. Stathmin expression was studied by immunohistochemistry in these tissue arrays. Stathmin expression was found to increase with Gleason Pattern in a statistically significant manner.

b) Study the consequence of stathmin overexpression or loss of expression on proliferation, migration and invasion using NeoTag1 and NeoTag2 cells.

Status: Stathmin expression has been successfully knocked down in NeoTag1 and NeoTag2 cells using SMARTpool siRNA from Dharmacon. In an article published in December 2005, Mistry et al. showed that knocking down stathmin expression in androgen-independent LNCaP cells caused a cell cycle arrest, induced apoptosis and suppressed clonogenic potential of the cells [1]. Performing the same experiments in the NeoTag cells would have been repetition. To avoid repetition, we knocked down stathmin and looked for other changes that might be occurring. Apart from the NeoTag1 and NeoTag2 cells, we knocked down stathmin in LNCaP, PC-3 and DU145 cells too. Surprisingly, in the DU145 cells, knocking down of stathmin induced an EMT (Epithelial to Mesenchymal Transition) like phenotype. Of the prostate cancer cell lines mentioned, DU145 is the only one that undergoes TGFβ induced EMT like phenotype. Knocking down stathmin sensitized the cells to TGFβ induced cellular morphology changes resulting in quicker EMT like phenotype. We found that stathmin may be modulating epithelial to mesenchymal transition of DU145 cells. Since this is a key event in invasion and subsequent metastasis in the tumor microenvironment, we postulate that stathmin may be involved in tumor metastasis. We evaluated the smad-dependent and -independent mechanisms of TGFβ activation in the context of EMT phenotype, and determined that stathmin modulates smad-independent

activity of TGFβ. In our knowledge, this is the first report establishing stathmin as a modulator of TGFβ activity.

Task 2

Determine which signaling pathway is activated through selective phosphorylation of stathmin and whether inactivation of this pathway promotes sensitization to treatment with Taxotere or Erbitux.

Status: Phosphoantibodies against specific serine residues of stathmin were used to study phosphorylation pattern in NeoTag1 and NeoTag2 cells. We also studied phosphorylation in LNCaP, PC-3 and DU145 cells. The small molecule kinase inhibitors failed to knock down stathmin phosphorylation in all cell lines tested. Hence as an alternative, we designed primers to generate phosphorylation site mutants to knock down stathmin phosphorylation in these cell lines. Generation of plasmids containing phosphorylation site mutant stathmin sequence and subsequent expression of these plasmids in the cells are pending. We also started investigating the mechanisms by which stathmin modultes the EMT phenotype in the DU145 cells. We have established that stathmin can modulate the MAPK pathway both in prostate (DU145) and breast (NMuMG) cells to initiate EMT development. This finding is significant as stathmin can then be potentially targeted for drug discovery to maintain a normal epithelial phenotype and control tumor spread. We have also identified p38MAPK as the first reported downstream effector of stathmin function in the prostate.

Task 3

Evaluate the effects of stathmin expression on tumor development and the outcomes of Taxotere, Erbitux treatment on blocking tumorigenesis and metastasis in tissue recombination and transgenic mouse models.

Status: Not yet started.

Summary of the Project
PCRP Predoctoral Traineeship Award
W81XWH-06-1-015
Stathmin: A "Relay Protein" in the Development of Prostate Cancer and a Potential Target for Anti-cancer Therapy
P.I. Ritwik Ghosh, PhD

Proteins which regulate normal development may promote tumorigenesis, tumor progression, or metastasis through dysregulation of these functions. We postulate that proteins, which regulate prostate growth also promote prostate cancer (PCa) progression. Stathmin was identified by two-dimensional gel electrophoresis and mass spectrometry. Stathmin levels increase early during normal mouse prostate development and again during prostate tumor development and progression [2]. In human prostate adenocarcinoma, stathmin increases in Gleason pattern 5 [2]. Further, stathmin is differentially phosphorylated in androgen-dependent LNCaP cells compared to androgen-independent PC-3 and DU145 cells [2]. This differential phosphorylation is modulated by androgen and anti-androgen treatment [2]. Hence, we have established that stathmin expression is highest when the prostate is undergoing morphogenesis or tumorigenesis and these processes may be regulated through differential phosphorylation. Furthermore, modulation of stathmin phosphorylation may correlate with the development of androgen-independent PCa.

The main tasks for the second year of this proposal have been 1) study the consequence of stathmin expression modulation on proliferation, migration and invasion using NeoTag1 and NeoTag2 cell and 2) determine whether modulation of stathmin activity can sensitize prostate cancer cells to treatment with Taxotere and Erbitux. Mistry et al., exhibited in December 2005 that knocking down stathmin expression in prostate

cancer cells caused a cell cycle arrest, induced apoptosis and suppressed clonogenic potential [1]. The same group published in 2006 that knockdown of stathmin sensitized LNCaP cells to treatment with Taxol and Etoposide [3]. The group again published in 2007 that stathmin downregulation sensitized endothelial cells to Taxol treatment [4]. In view of these publications, it would have been repetitive to do the same experiments in NeoTag cells. So, we started investigating the biological effect of knocking down stathmin in prostate cancer cells. We used SMARTpool siRNA to knock down stathmin expression in PC-3, LNCaP, BPH and DU145 cells. Interestingly we saw that knocking down stathmin induces a cell shape change in DU145 cells. Unpublished data from our lab shows that of the cell lines mentioned above, only DU145 undergoes EMT upon TGFβ treatment (Fig. 1 and 2). Stathmin downregulation resulted in an epithelial-to-mesenchymal transition (EMT) like phenotype in the DU145 cells (Fig. 2).

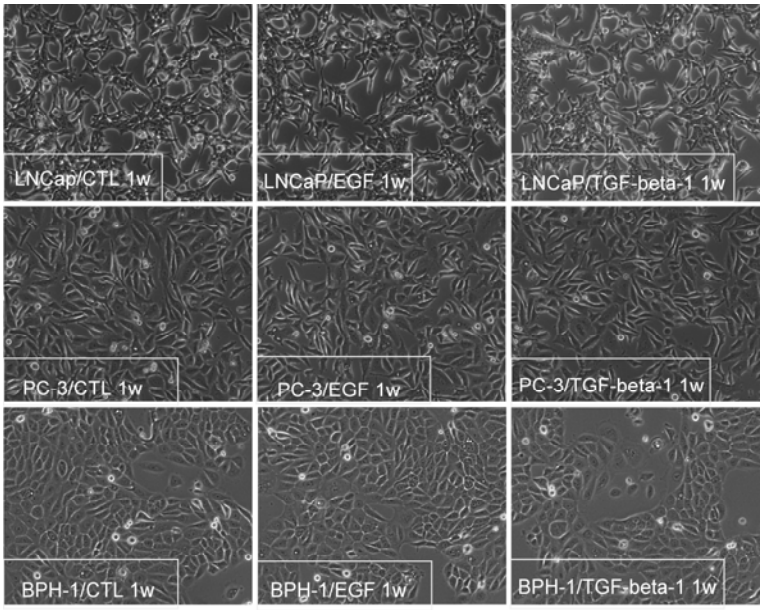

Figure 1. TGFβ induced EMT in PCa cells. LNCaP, PC-3 and BPH cells were treated with 5ng/ml and 10ng/ml TGFβ and EGF respectively, alone or in combination for 7 days. EMT was not observed in any of these cell lines. **(Unpublished Data)**

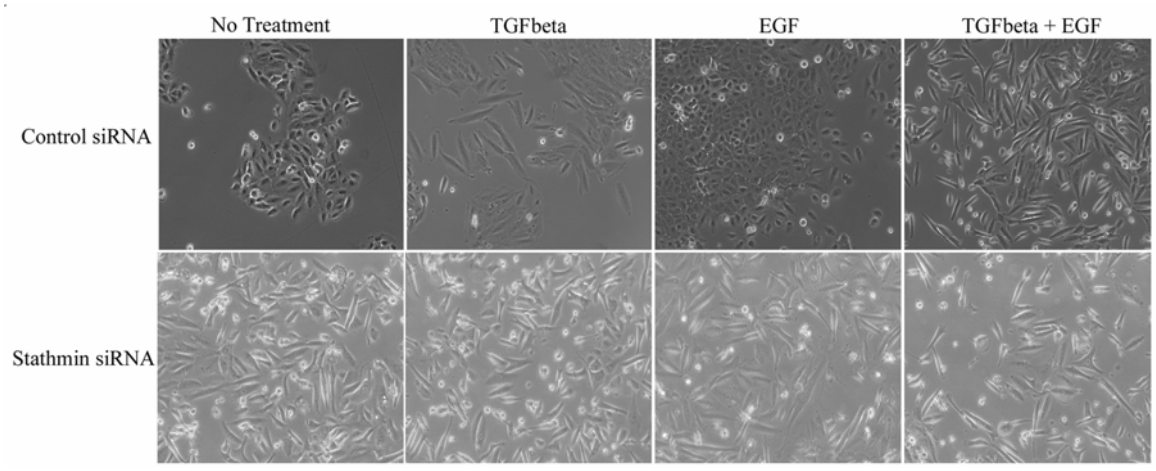

Figure 2. RNAi mediated downregulation of stathmin induces EMT in DU145 cells without TGFβ treatment. SMARTpool siRNA was used to knock down stathmin. Cells transfected with non-targeting control siRNA, requires 7 days of TGFβ treatment to elicit EMT phenotype. However, cells transfected with stathmin siRNA exhibit EMT within 24 hours and without TGFβ treatment. **(Unpublished Data)**

When stathmin is knocked down, EMT cells appear spontaneously within 1 day and without TGFβ treatment (Fig. 2). In contrast, cells transfected with non-targeting control siRNA require 7 days of TGF-β1 treatment to undergo EMT (Fig. 2). Immunnocytochemical (Fig. 3 Panel A)and western blot analysis (Fig. 3 Panel B) exhibits that knockdown of stathmin resulted in increased expression of mesenchymal marker vimentin and a concomitant decrease in epithelial marker, E-cadherin (Fig 3 Panels A & B). Downregulation of E-cadherin was also accompanied with a downregulation of p120 suggesting that E-Cadherin, Vimentin and p120 levels are modulated by stathmin (Fig 3 Panels A).

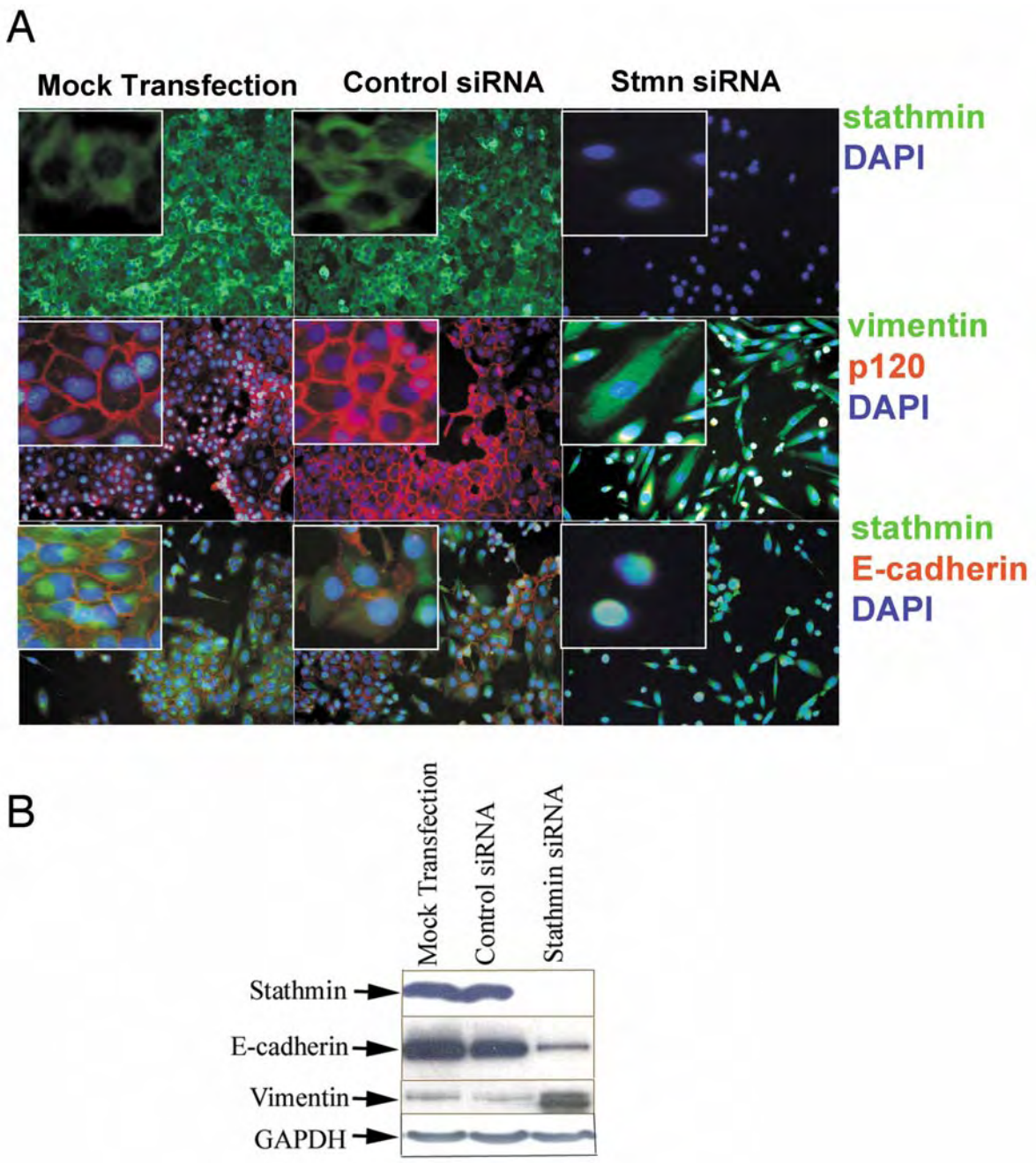

Figure 3. Stathmin downregulation in DU145 cells results in EMT-like cells with decreased E-cadherin and increased vimentin expression. A. Immunofluorescence analysis reveals decreased E-cadherin and p120 and increased vimentin expression in DU145 cells transfected with stathmin siRNA. Mock transfection and non-targeting control siRNA transfection does not affect E-cadhein, p120 and Vimentin expression. B. Western blot analysis to confirm stathmin downregulation in cells transfected with stathmin siRNA. Donwregulation of E-cadherin and up-regulation of vimetin in siRNA transfected cells is also confirmed. **(Unpublished Data)**

Smad molecules are effectors of TGFβ signaling in the cell. As discussed in Chapter V, binding of the ligand to TGFβ Receptor Type II leads to the recruitment of TGFβ Receptor Type I and results in active receptor ligand complex. Subsequently, Smad2 and Smad3 is phosphorylated, to complex with Smad4, for subsequent translocation into the nucleus to activate transcription of target genes such as slug and snail. TGFβ can elicit the EMT phenotype through either a smad -dependent or – independent mechanim. The smad-dependent mechanism leads to the activation of genes such as snail and slug, which represses E-cadherin expression. The smad-independent mechanism can involve a number of molecules such as p38MAPK, RhoA, p160ROCK etc., and also suppress E-cadherin expression. We sought to identify which of these pathways is being modulated by stathmin in EMT. DU145 cells transfected either with control siRNA or with stathmin siRNA were treated with increasing concentrations of human recombinant TGF-β1 (0, 0.1, 0.5, 2.0, 5.0ng/ml) (Fig. 4 Panel A). Smad2 and Smad3 phosphorylation was studied by western blot analysis with antibodies raised against specific phospho-forms of Smad molecule (Fig. 4 Panel A). Interestingly, phosphorylated levels of Smad2 and Smad3 are similar at all concentrations tested irrespective of the presence or absence of stathmin expression (Fig. 4 Panel A). Since phospho-Smad2/3 levels were highest at 5.0ng/ml of TGF-β1, DU145 cells were treated with this concentration for 0, 1, 2, 4 and 8 hours to determine the effects of stathmin expression on Smad2 and Smad3 phosphorylation over time (Fig. 4 Panel B). Irrespective of stathmin expression levels, TGF-β1 treatment caused Smad2 and Smad3 phosphorylation to increase with time up to 2 hours, after which it gradually decreased till no phosphorylation could be detected at 8 hours (Fig. 4 Panel B). These results

indicate that stathmin regulates the TGF-β1-mediated EMT formation through a smad-independent mechanism.

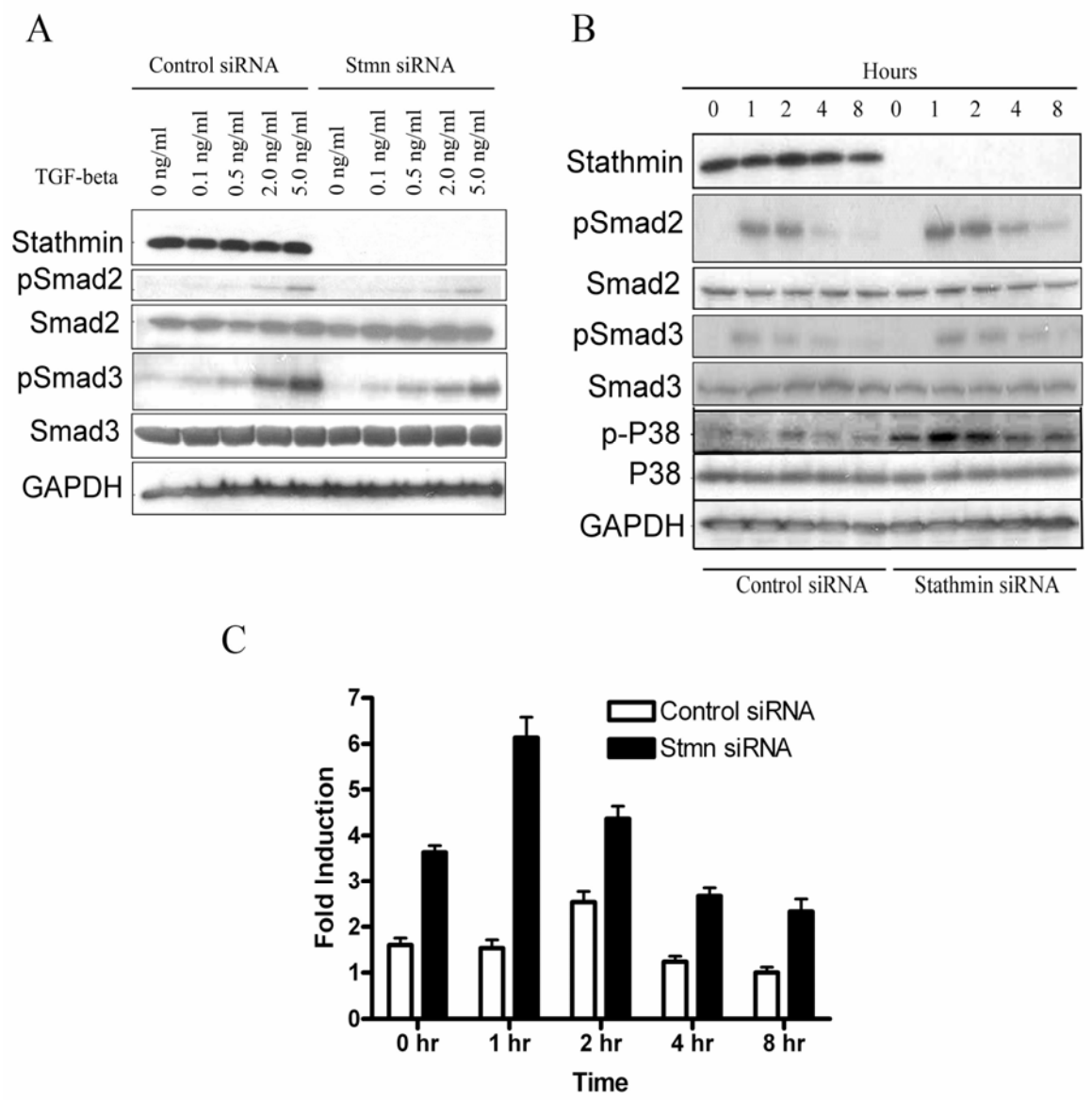

Figure 4. TGFβ-induced Smad2/3 and P38 phosphorylation in DU145 cells transfected with control or stathmin siRNA. A. Smad2 and Smad3 phosphorylation increases with increasing concentration of TGFβ (0-5ng/ml). Phosphorylation levels are similar in control- or stathmin-siRNA transfected cells. B. Smad2 and Smad3 phosphorylation is maximal after 1 hr of treatment with 5ng/ml TGFβ both in control- and stathmin-siRNA transfected cells. Phosphorylation at other time points are also similar between the two groups implying stathmin does not affect Smad phosphorylation. P38 phosphorylation at all time points is higher in stathmin-siRNA transfected cells, implying that stathmin downregulation can activate p38. C. Densitometric analysis reveals that stathmin downregulation results in a 4-fold induction in P38 phosphorylation in stathmin-siRNA cells compared to control-siRNA cells after 1 hr of TGFβ treatment. **(Unpublished Data)**

We next sought to determine if stathmin could modulate p38MAPK activity to elicit the EMT phenotype. TGFβ treatment has been reported to increase p38 phosphorylation in a time-dependent manner. As described earlier, DU145 cells transfected with control/stathmin siRNA were treated with 5.0ng/ml TGF-β1 for 0, 1, 2, 4 and 8 hours (Fig. 26 Panel B) and p38 phosphorylation was studied by western blot analysis with an antibody that recognizes phosho-p38. p38 appears to be constitutively phosphorylated in stathmin siRNA-transfected DU145 cells, even in the absence of TGF-β1 treatment (Fig. 4 Panel B). Furthermore, p38 is maximally phosphorylated after 1hour (~4-fold compared to time 0 hour) (Fig. 4 Panel C) of TGF-β1 treatment and phospho-p38 decreases to basal levels by 4 hour. In contrast, phospho-p38 levels increased minimally at 2 hours post treatment in cells transfected with control siRNA. In cells transfected with stathmin siRNA, p38 phosphorylation was higher at all time-points tested compared to cells transfected with control siRNA (Fig. 4 Panel B and C).

These observations suggest that stathmin modulates p38 activity during EMT. If stathmin regulates EMT formation by modulating p38 activity, then inhibiting p38 phosphorylation should inhibit/delay appearance of EMT in DU145 cells transfected with stathmin siRNA. To test this hypothesis, we used the small molecule kinase inhibitor SB203580 to block p38 phosphorylation in DU145 cells transfected with stathmin or control siRNA (Fig. 5 Panels A and B). SB203580 has been reported to specifically block p38 phosphorylation. As described earlier, cells transfected with stathmin siRNA undergo EMT within 24 hours. In contrast, DU145 cells transfected with stathmin siRNA, but treated with SB203580 failed to transition into spindle-shaped cells indicative of the

EMT phenotype (Fig. 5 Panel A). Western blot analysis confirms that p38 phosphorylation was inhibited by SB203580 (Fig. 5 Panel B). Double immunofluorescence was performed to determine the effects of inhibiting p38 phosphorylation on cell phenotype (Fig. 6). In stathmin siRNA-transfected DU145 cells treated with SB203580, E-cadherin is re-expressed and vimentin expression is lost resulting in the restoration of the epithelial phenotype (Fig. 6). These data substantiate the observation that stathmin regulates TGF-β-mediated EMT by modulating p38MAPK activity.

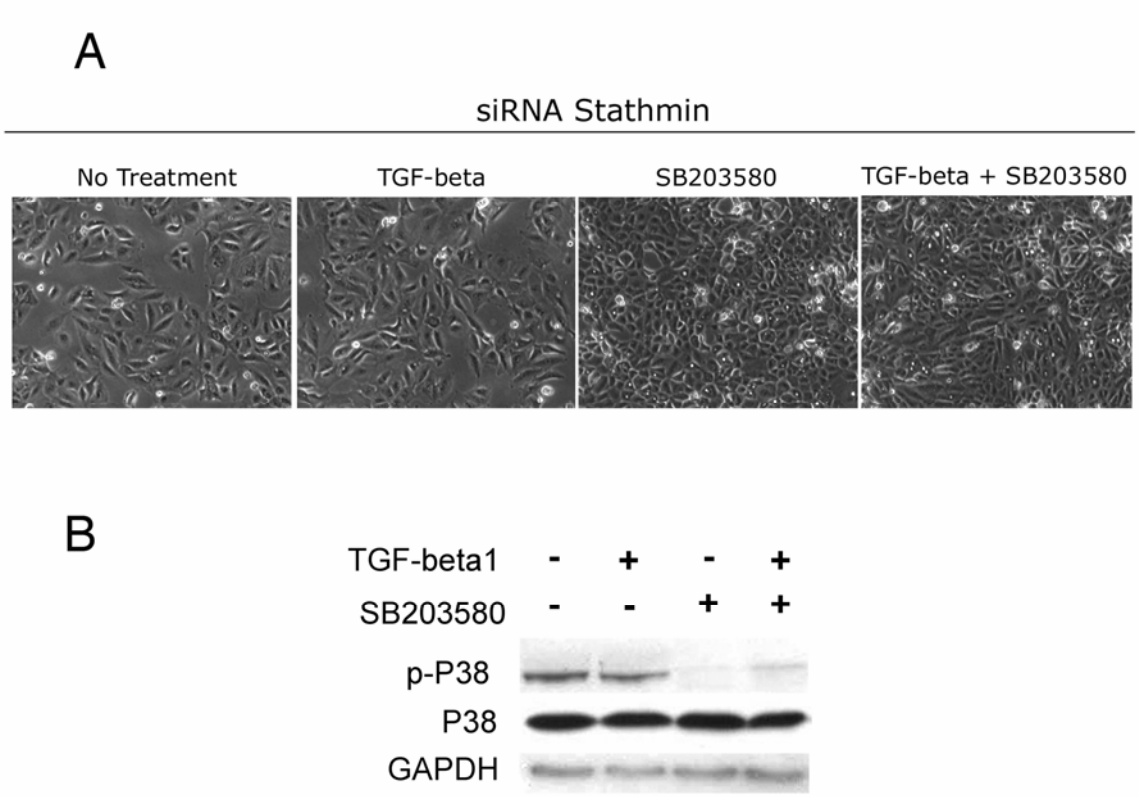

Figure 5. Blocking P38 activity inhibits EMT phenotype in stathmin-siRNA transfected DU145 cells. A. DU145 cells transfected with stathmin siRNA were treated with TGFβ and SB203580, either alone or in combination. Untreated cells and cells treated with TGFβ exhibit EMT phenotype within 24 hours of siRNA transfection. However cells treated with SB203580 alone or in combination with TGFβ do not undergo EMT. B. Western blot analysis to confirm that treatment with SB203580 results in downregulation of p38 phosphorylation. p38 levels do not change with treatment and GAPDH has been used to ensure equal loading in all the lanes. **(Unpublished Data)**

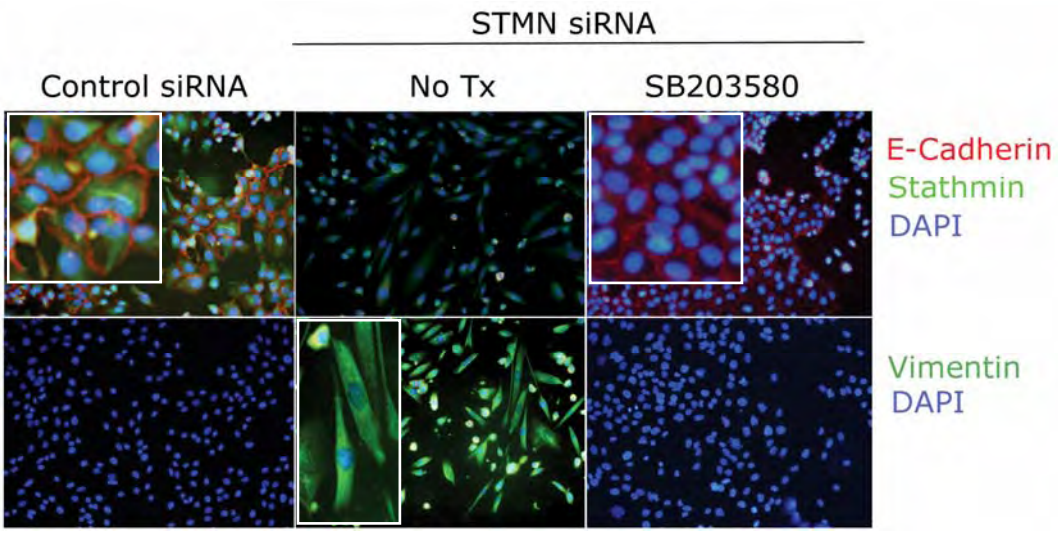

Figure 29. Inhibiting p38 phosphorylation restores epithelial phenotype in DU145 cells transfected with stathmin-siRNA. Cells transfected with control siRNA express E-cadherin and stathmin but do not express Vimentin. Cells transfected with stathmin siRNA express Vimentin but do not express E-cadherin and stathmin. However, inhibiting P38 activation by using SB203580 results in the reexpression of E-cadherin and downregulation of Vimentin, implying epithelial phenotype is restored in absence of stathmin. **(Unpublished Data)**

Research Goals/Training Accomplishments

1) In-depth immunohistochemical and statistical analyses on a tissue array containing prostate tissue samples from human BPH and prostate cancer patients.
2) RNA interference technology to knock down stathmin in a variety of human and mouse prostate cancer cell lines.
3) Designing primers to introduce site –directed mutagenesis to generate hyper- and hypo-phosphorylated stathmin.
4) Completion of PhD degree.

Reportable Outcomes

1) Peer-reviewed publication

   a) **Increased expression and differential phosphorylation of stathmin may promote prostate cancer progression.** *Ritwik Ghosh, Guangyu Gu, Erin Tillman, Jialing Yuan, Yongqing Wang, Ladan Fazli, Paul S. Rennie, Susan Kasper.* Prostate. 2007 Jul 1;67(10):1038-52. PMID: 17455228

2) Manuscript in preparation

   a) Stathmin modulates TGFβ mediated EMT formation in prostate cancer cells.

Conclusions

In summary, we propose that stathmin is a regulator of epithelial cell homeostasis. Stathmin may exhibit differential function in normal compared to cancer cells, similar to the duel roles of TGF-β as a tumor suppressor in normal cells and a tumor promoter at later stages of cancer progression. Stathmin over-expression has been associated with a number of different cancers including leukemia as well as breast, ovarian and prostate cancer. Immunohistochemical studies reveal that increased stathmin protein levels correlate positively with poor outcome. On the other hand, mechanisms, which disrupt stathmin expression, such as activation of TGF-β1 signaling, result in destabilization of the cytoskeletal framework of the epithelial cell and progression to EMT. This observation is apparently counter-intuitive, since EMT has been associated with

progression to a more aggressive tumor phenotype leading to invasion and metastasis. Thus, on one hand, increased stathmin expression correlates with high grade prostate cancer and on the other hand inhibition of stathmin expression can potentially make the tumor more aggressive. One possibility is downregulation of stathmin expression is required for transformation into more motile EMT cells, which now metastasize to distant organs. Once the invading cells home to a distant organ they may undergo the reverse mesenchymal-to-epithelial transition (MET), re-express stathmin, and grow as epithelial cells. Thus, stathmin represents an attractive target for therapeutic intervention aimed at maintaining a normal epithelial phenotype and controlling tumor spread.

References

1. Mistry S.J., Bank A., and Atweh G.F. Targeting stathmin in prostate cancer. Molecular Cancer Therapeutics. 2005;4(12):1821-1829.
2. Ghosh R, Gu G, Tillman E, Yuan J, Wang Y, Fazli L, Rennie P.S., Kasper S. Increased expression and differential phosphorylation of stathmin may promote prostate cancer progression. Prostate. 2007 Jul 1;67(10):1038-52.
3. Mistry SJ, Atweh GF. Therapeutic interactions between stathmin inhibition and chemotherapeutic agents in prostate cancer. Molecular Cancer Therapeutics. 2006 Dec;5(12):3248-57.
4. Mistry SJ, Bank A, Atweh GF. Synergistic antiangiogenic effects of stathmin inhibition and taxol exposure. Molecular Cancer Therapeutics. 2007 Aug;5(8):773-82.

The Prostate 67:1038 – 1052 (2007)

Increased Expression and Differential Phosphorylation of Stathmin May Promote Prostate Cancer Progression

Ritwik Ghosh,[1,2] Guangyu Gu,[1] Erin Tillman,[1,2] Jialing Yuan,[1] Yongqing Wang,[1] Ladan Fazli,[3] Paul S. Rennie,[3] and Susan Kasper[1,2]*

[1]*Department of Urologic Surgery, Vanderbilt University Medical Center, Nashville, Tennessee*
[2]*The Vanderbilt-Ingram Cancer Center, Nashville, Tennessee*
[3]*The Prostate Cancer Center at Vancouver General Hospital, University of British Columbia, British Columbia, Canada*

BACKGROUND. Proteins which regulate normal development may promote tumorigenesis, tumor progression, or metastasis through dysregulation of these functions. We postulate that proteins, which regulate prostate growth also promote prostate cancer (PCa) progression.
METHODS. Two Dimensional Gel Electrophoresis was utilized to compare patterns of protein expression in 12T-7f prostates (LPB-Tag mouse model for PCa) during tumor development and progression with those of normal developing and adult wild type CD-1 prostates. Stathmin expression and phosphorylation patterns were analyzed in mouse and human PCa cell lines as well as in human PCa tissue arrays.
RESULTS. Stathmin was identified by two-dimensional gel electrophoresis and mass spectrometry. Stathmin levels increase early during normal mouse prostate development and again during prostate tumor development and progression. In human prostate adenocarcinoma, stathmin increases in Gleason pattern 5. Further, stathmin is differentially phosphorylated in androgen-dependent LNCaP cells compared to androgen-independent PC-3 and DU145 cells. This differential phosphorylation is modulated by androgen and anti-androgen treatment.
CONCLUSION. Stathmin expression is highest when the prostate is undergoing morphogenesis or tumorigenesis and these processes may be regulated through differential phosphorylation. Furthermore, modulation of stathmin phosphorylation may correlate with the development of androgen-independent PCa. *Prostate 67: 1038–1052, 2007.*

KEY WORDS: **stathmin; tumorigenesis; prostate cancer; prostatic intraepithelial neoplasia (PIN); adenocarcinoma; tissue recombination**

INTRODUCTION

Multiple molecular events control prostate cancer initiation, growth, invasion, and metastasis. In spite of the prevalence of PCa, our understanding of the genetic alterations occurring during these processes is limited. In normal mouse prostate development, prostatic bud commitment occurs at embryonic day 16 when signaling centers develop and subsequently invade the mesenchymal pad and induce epithelial cell elements [1,2]. At birth, prostatic buds are rudimentary and morphogenesis of these structures occurs primarily in the postnatal period from 1 to 5 weeks (wks) of age when outgrowth ceases and maturation of the prostate gland is complete [1,2]. At 6 weeks of age, the animal is

*Correspondence to: Susan Kasper, Department of Urologic Surgery, A-1302 Medical Center North, Vanderbilt University Medical Center, 1161 21st Avenue South, Nashville, TN 37232-2765.
E-mail: susan.kasper@vanderbilt.edu
Received 9 January 2007; Accepted 8 March 2007
DOI 10.1002/pros.20601
Published online 23 April 2007 in Wiley InterScience (www.interscience.wiley.com).

sexually mature and mitotic cells are typically not observed in the growth quiescent adult prostate [1,2]. Numerous prostate cancer models have been generated by disrupting the expression of a gene of interest in transgenic mice [3]. Typically, epithelial cells proliferate and develop into lesions ranging from hyperplasia to low- and high-grade intraepithelial neoplasia (LGPIN and HGPIN, respectively), locally invasive carcinoma and/or metastases. Reactive stromal proliferation is also observed [3].

Several developmentally regulated proteins have been implicated in the tumorigenic process. For example, the Nkx3.1 homeobox gene is an early marker of prostate epithelium during embryogenesis and is expressed at all stages of prostate differentiation [4,5]. The adult prostate continues to express Nkx3.1 and loss of expression promotes prostatic epithelial hyperplasia and dysplasia, which increase in severity with age [4,5]. Notch-1, another developmental protein, is expressed more highly in early postnatal than in adult prostate and is required during branching morphogenesis, growth, and differentiation [6,7]. Inactivation of Notch enhances proliferation and impairs differentiation of prostatic epithelial cells. Downregulation of Notch-1 and Hey-1 expression is also observed in human prostate adenocarcinoma samples [6,7]. Sonic hedgehog (Shh) is expressed in developing prostatic epithelium and activates Gli-1 expression in adjacent mesenchyme to promote branching morphogenesis [8]. Shh signaling is not restricted to development, being detected in normal and prostate cancer tissues. In the LNCaP xenograft tumor model, Fan and co-workers demonstrated that overexpression of Shh in LNCaP cells increased Gli-1 expression in adjacent tumor stroma and promoted tumor growth [8].

In the present study, we used two-dimensional gel electrophoresis to identify proteins, which may promote PCa development. This proteomics approach allowed us to compare protein expression profiles in control CD-1 developing and adult prostates with those in 12T-7f prostate tumors. Earlier, we had generated the LPB-Tag transgenic model by using a 10.8 kb rat probasin promoter region to target SV40 large T antigen (small t antigen is deleted) to the mouse prostate [9,10]. The 12T-7f prostate tumors develop in parallel with sexual maturation, since large T antigen gene is under control of the androgen-regulated probasin promoter. Tumors continue to exhibit a high proliferative index, PIN and localized adenocarcinoma; however, metastasis is rarely seen [10,11]. Using this model, we identified the phosphoprotein stathmin.

Stathmin is a 148 amino acid ubiquitous cytosolic phosphoprotein whose nomenclature also includes p19 [12], prosolin [13], Lap18 [14], metablastin [15], and Oncoprotein 18 or Op18 [16]. Overexpression of stathmin has been associated with leukemia, breast, and ovarian cancer [16–23]. The functions of stathmin can be broadly classified as: (a) regulation of microtubule dynamics [24] and (b) non-microtubule functions which include: (i) regulation of prolactin, and (ii) regulation of muscle cell differentiation by growth factors, hormones and neurotransmitters [25].

Stathmin is a highly conserved protein and the N-terminal contains four serine residues which are phosphorylated by diverse groups of extracellular factors in mammalian cells [26], suggesting that stathmin participates as a ''relay protein'' in several intracellular signaling pathways [25]. The first pathway involves PAK1 and Ca^{2+}/calmodulin-dependent kinase which phosphorylate stathmin at serine 16 (Ser16) [27]. Phosphorylation by PAK1 requires Rac/Cdc42 and has been shown to inhibit stathmin-induced destabilization of microtubules, thereby regulating F-actin and microtubule dynamics [27,28]. The second pathway involves mitogen-activated protein (MAP) kinase ERK2 which when triggered by growth factor receptors, phosphorylates stathmin at Ser25 [29,30]. A Ser25 to alanine mutation blocks phosphorylation and inhibits cell growth in leukemic K562 cells [23]. A third pathway involves cyclin-dependent kinase 1 (CDK1) which phosphorylates stathmin at Ser38 [31]. Inhibition of Ser38 phosphorylation blocks cell division and induces a G_2/M block in K562 cells [32]. Phosphorylation of stathmin at Ser63 by Protein Kinase A (PKA) represents the fourth pathway [33] and a Ser63 to alanine mutation which prevents phosphorylation at this residue results in microtubule destabilization and a cell cycle arrest in K562 cells [34,35]. At this time, it is not clear which of these pathways is involved in promoting PCa.

Our study demonstrates that postnatally, stathmin expression is high in prostatic epithelium and declines as the prostate differentiates into a growth quiescent gland. Stathmin expression is elevated again during PCa development and continues to be expressed during PCa progression. Analyses of archival human prostate tissue sections indicate that stathmin is initially expressed in the basal cell compartment in Benign Prostatic Hyperplasia (BPH), whereas stathmin is overexpressed in luminal epithelial cells in PIN and continues to be expressed in adenocarcinoma. Furthermore, differential stathmin phosphorylation is observed in androgen-independent PC-3 and DU145 cells compared to androgen-dependent LNCaP cells, suggesting that stathmin activity is modulated with PCa progression. Understanding which pathways stathmin regulate is imperative to identifying potential targets for treatment of PCa.

MATERIALS AND METHODS

Animals and Tissues

CD-1 and LPB-Tag 12T-7f mice on a CD-1 background were housed in the animal care facility at Vanderbilt University Medical Center in accordance with the National Institutes of Health (NIH) and institutional guidelines for laboratory animals. CD-1 males and females were purchased from Harlan (Indianapolis, IN). The 12T-7f mouse model for prostate cancer has been described in detail elsewhere [9,10]. This model was generated by utilizing the long probasin promoter (−10,806 to +28 bp, LPB) to target the Large T antigen (*Tag*) gene to the mouse prostate. Small t-antigen is not expressed in this model. Tumor incidence is 100% in mice heterozygote for the LPB-Tag transgene and Tag expression occurs specifically in prostate epithelial cells. Tumor growth is rapid, histologically containing PIN and localized adenocarcinoma. CD-1 as well as 12T-7f mice were bred to provide normal CD-1 and 12T-7f prostates at 1, 2, 3, 4, 5, 6, 10, 15, and 40 weeks of age. The number of CD-1 prostates dissected for the early times points were approximately 900 for 2 weeks, 450 for 3 weeks, and 300 for 4 weeks of age, resulting in a total of 1,650 mouse dorsal lobes dissected. The CD-1 dorsal prostates were pooled into three groups of 300 for 2 weeks, 150 for 3 weeks of age, and 100 for 4 weeks of age. The same number of prostates was dissected for the 12T-7f mice, kept separate until genotyping was completed and then separated into three pools for each time point as described above. As age increased, the prostatic lobes were larger and the number of prostates required per group decreased. All data presented is generated from the dorsal prostate (DP). For immunohistochemical analysis, individual prostatic lobes were fixed in 10% buffered formalin and subjected to standard processing and paraffin embedding.

Cell Culture

DU145 cells were cultured in MEM media (Gibco, Grand Island NY)) supplemented with 10% FBS (Hyclone, Logan UT), 2 mM glutamine (Gibco), 0.1 mM non-essential amino acid (Gibco) and 1.0 mM sodium pyruvate (Gibco). PC-3 cells were cultured in F-12K Nutrient mixture supplemented with 10% FBS. LNCaP cells were cultured in RPMI 1640 media supplemented with 10% FBS, 1.25 g/500 ml of Glucose and 1.0 mM sodium pyruvate. BPH1 cells were cultured in RPMI 1640 media supplemented with 5% FBS. NeoTag cells were cultured as described previously [36]. HeLa and HeLa-AR cells were cultured in low glucose DMEM (Gibco) supplemented with 10% FBS. For the androgen and anti-androgen treatments, LNCaP cells were cultured in 24-well plates at a density of 10^5 cells/well and upon reaching 80% confluency were treated with androgens and anti-androgens. Cells were harvested 24 hr later in RIPA buffer and processed for Western blot analysis as described below.

Western Blot Analysis

Cell proteins were isolated using RIPA buffer and concentration determined using the BCA™ Protein Assay Kit (Pierce, Rockford IL). Total protein (20 μg) were separated by hand cast 12% sodium dodecyl sulfate polyacrylamide gel electrophoresis (SDS–PAGE) and transferred onto Hybond™ ECL™ Nitrocellulose membranes (Amersham Pharmacia Biotech, Uppsala, Sweden). The membranes were blocked with 5% skim milk (BD, Sparks, MD) and incubated with a 1:1,000 dilution of rabbit polyclonal anti-stathmin antibody (Cell Signalling Technology, Boston, MA) or a rabbit polyclonal anti-p-Ser16-stathmin/rabbit polyclonal anti-p-Ser63-stathmin (Santa Cruz Biotechnology, Santa Cruz, CA)/rabbit polyclonal anti-p-Ser25-stathmin/rabbit polyclonal anti-p-Ser38-stathmin (gift from Dr. Andre Sobel, Paris). Membranes were washed and incubated with 1:10,000 dilution of horseradish peroxidase-linked anti-rabbit IgG (Amersham Pharmacia Biotech). Proteins were visualized in ECL-plus solution (Amersham Pharmacia Biotech, Uppsala, Sweden) and exposed on Hyperfilm™ ECL™ (Amersham Pharmacia Biotech) for 3–5 min. To ensure equal amount of protein was loaded in each lane, the membrane was stripped using 100 mM 2-mercaptoethanol, 2% SDS, 62.5 mM Tris-HCL for 30 min at 70°C, washed, blocked, and subjected to immunodetection as outlined above using mouse polyclonal anti-GAPDH (1:5,000) as primary antibody (IMGENEX, San Diego, CA).

Real-Time RT-PCR Analysis

Stathmin mRNA levels in developing and in adult CD-1 prostates were compared to those in 12T-7f mouse tumors. cDNA was generated from 2 μg total RNA from 1, 2, 3, 4, 5, 6, and 10-week CD-1 and 12T-7f prostates and used in PCR reactions to determine stathmin expression levels. The following primers with an annealing temperature of 58°C were used in the PCR reaction: forward primer, 5′-CACCATGGCTTCTTCTGATATCCAGG-3′; reverse primer, 5′-AAATTAGTCAGCTTCAGTCTCGTCAGC-3′. The standard curve was generated using serial dilutions of pGEM-TEasy-Stathmin plasmid containing full-length stathmin cDNA. The human 18S gene was subcloned into pGEM-TEasy (Promega) and served as internal standard. PCR amplification was performed using SYBR Green PCR Core Reagent (Applied Biosystems, Foster

City, CA), followed by analysis of melting curves to validate the real-time RT-PCR data and agarose gel electrophoresis of an aliquot from each RT-PCR product to monitor purity of the specific RT-PCR product. Stathmin concentrations (in μM) were determined and standardized to the 18S product from the same sample.

Gleason PatternTissue Microarray (TMA)

Slides (H&E) from radical prostatectomy specimen (from 1989 to 2003) were obtained from the Vancouver General Hospital. The patients had no prior treatment. Benign and cancer lesions were identified and marked in donor paraffin blocks using matching H&E reference slides. The TMA was constructed using a manual tissue micro arrayer (Beecher Instruments, Silver Spring, MD). Each marked block for benign and cancer was sampled 4 times with a core diameter of 0.6 mm arrayed in rectangular pattern with 1 mm between the centers of each core, creating a quadruplet TMA layout which was arrayed by increasing Gleason pattern from 3 to 5 (Table I). To score stathmin staining, the number of stathmin positive cells per each core were counted and the cores from each patient averaged and graphed. A total of 4 cores/patient or 200 cores from 50 patients were included in the TMA.

Immunohistochemistry (IHC) and Immunofluorescence (IF) Microscopy

Archival human prostate specimens as well as CD-1 and 12T-7f mouse prostate samples were formalin-fixed and paraffin-embedded. Five micron tissue sections were cut, deparaffinized and subjected to antigen retrieval by immersing the slides in Antigen Unmasking Solution (Vector Laboratories, Burlingame, CA), microwaving for 10 minutes and allowing the slides to cool to room temperature in the buffer. The slides were then washed twice in distilled water prior to IHC analysis. Slides were incubated with a 1:50 dilution of rabbit polyclonal anti-stathmin antibody (Cell Signaling Technology, Boston, MA) for standard IHC analysis and a combination of anti-stathmin and monoclonal mouse anti-p63 antibody (NeoMarkers, Fremont, CA) for double IF microscopy overnight at 4°C. For standard IHC, sections were processed and developed using DakoCytomation LSAB®+ System-HRP (Dako North America Inc., Carpinteria, CA). The sections were counterstained with hematoxylin, dehydrated and mounted with Permount® (Fisher Scientific, Hampton, NH). For double IF analysis, sections were blocked using 3% donkey serum and 3% BSA in phosphate buffered saline (PBS). After incubating with primary antibodies, sections were washed and incubated with donkey anti-rabbit Alexa Fluor 488 (green) and donkey anti-mouse Alexa Fluor 594 (red) (Molecular Probes) secondary antibodies to detect stathmin and p63 respectively. Sections were washed and mounted in Vectashield® mounting medium containing DAPI (Vector Laboratories, Burlingame, CA). All digital images were captured using the Zeiss Axiovision Camera and software attached to a Zeiss Imager M1 microscope. The Tissue Microarray was stained for stathmin utilizing the Discovery XT Autostainer (Ventana Medical System Inc, Tuscan Arizona) and DABMap.

TABLE I. Tissue Array Representing BPH and PCa

Histopathology of specimen	Number of patients
BPH	12
Gleason Pattern 3	12
Gleason Pattern 4	10
Gleason Pattern 5	16
Total	50

A total of 4 cores/patient or 200 cores from 50 BPH and PCa patients were arrayed in sequential order from Gleason pattern from 3 to 5.

Two-Dimensional Gel Electrophoresis and Mass Spectrometry

Tissue proteins were extracted in lysis buffer (7 M urea, 2 M thiourea, 4% CHAPS, 30 mM Tris, 5 mM magnesium acetate). One hundred micrograms of protein from 3 wk developing CD-1 prostates, 15 wk adult CD-1 prostates and 15 wk 12T-7f prostate tumors were labeled with 200 picomoles of Cy2, CY3, or Cy5 (Amersham Biosciences, Piscataway, NJ) respectively for 30 minutes on ice in the dark. Samples were treated with 2 μl of 10 mM lysine for 10 minutes on ice in the dark to quench the reactions. The three samples were then combined and added to an equal volume of 2× rehydration buffer (7 M Urea, 2 M thiourea, 4% CHAPS, 4 mg/ml DTT) supplemented with 0.5% immobilized pH gradient (IPG) buffer 4–7. Standard 2D gel electrophoresis was performed using an IPGphor first-dimension isoelectric focusing unit and 24 cm 4–7 IPG strips (Amersham Biosciences, Piscataway, NJ) to co-resolve combined samples labeled with Cy2/3/5. The samples were reduced and alkylated with 1% DTT and 2.5% iodoacetamide in equilibration buffer (6 M urea, 30% glycerol, 2% SDS, 50 mM Tris pH 8.8) before second dimension separation on a 12% SDS-PAGE using an Ettan DALT 12 unit (Amersham Biosciences, Piscataway, NJ). Hand-cast SDS-PAGE gels were used for second dimension separation using low fluorescence glass plates, with one glass plate

presilanized (bind-silane, Amersham Biosciences, Piscataway, NJ) to affix the polymerized gel to only one of the glass plates.

CyDye-specific images were acquired in the 2D 2920 Master Imager (Amersham Biosciences, Piscataway, NJ) using mutually exclusive excitation/emission wavelenths. DeCyder Differential In-gel Analysis software (Amersham Biosciences, Piscataway, NJ) was used to calculate individual protein spot volume ratios. Mean values were calculated from a modeled normal distribution of all spot volume relations. Two standard deviations calculated from the mean were used to identify protein spot features with significant abundance changes within the 95% confidence interval.

2D-gels were stained with Sypro Ruby Red (Molecular Probes) according to the manufacturer's protocol. Proteins of interest were robotically excised and digested in-gel with trypsin protease (Promega) using Ettan Spot Picker and Digester Workstations (Amersham Biosciences, Piscataway, NJ). Peptides were reconstituted in 10 μl of 0.1% trifluoroacetic acid. C18 ziptip pipette tips (Millipore, Billerica, MA) were used to desalt/concentrate into 2 μl of 60% acetonitrile and 0.1% trifluoroacetic acid. A Voyager 4700 (Applied Biosystems) was used to perform Matrix-assisted laser desorption/ionization, time-of-flight (MALDI-TOF) mass spectrometry. Peptide mass maps, acquired in reflectron mode averaging 2,000 laser shots per spectrum, were internally calibrated to within 20 ppm mass accuracy using trypsin autolytic peptides ($m/z = 842.51$, 1045.56, and 2211.10). MASCOT (www.matrixscience.com) and ProFound (prowl.rockefeller.edu) database search algorithms were used to interrogate human sequences in the SWISS-PROT and NCBInr databases respectively. Masses of tryptic peptides were used to identify proteins from MALDI-TOF. The search algorithm allowed for carbamidomethylation of cysteine, partial oxidation of methionic residues and one missed trypsin cleavage.

Tissue Recombination Assay

Tissue recombination experiments using NeoTag cells were performed as previously described [36]. Briefly, 100,000 epithelial (NeoTag) and 300,000 mesenchymal (rat embryonic urogenital mesenchyme (UGM)) cells were combined in suspension. The cell mixtures were pelleted and reconstituted in 50 μl of neutralized type I rat tail collagen prepared as described previously. Recombinants were incubated at 37°C for 15 min to allow solidification of the collagen plug and subsequently incubated in RPMI 1640 medium supplemented with 5% FBS at 37°C overnight and grafted under the renal capsule of male athymic nude mice. NeoTag cells without UGM were used as control recombinants. After 4 weeks, mice were euthanized and tissue recombinants were dissected and processed for immunohistochemistry by standard methods.

RESULTS

Stathmin Expression Is Upregulated During Prostate Morphogenesis and Tumorigenesis

In the present study, we used two-dimensional gel electrophoresis to identify proteins, which may be involved in promoting PCa development. Our approach was to compare periods in which prostate growth is highest to those in which the prostate is growth quiescent. Since normal prostate development continues postnatally up to 5 weeks of age, we selected the 3 week normal CD-1 prostates as representative of active prostatic development. Fifteen week CD-1 prostates were chosen to represent mature growth quiescent glands since few, if any, proliferating cells can be detected. The LPB-Tag line 12T-7f mouse PCa model was selected since these tumors undergo rapid proliferation and develop PIN with limited localized adenocarcinoma lesions. Protein lysates were prepared from 3 and 15 weeks CD-1 dorsal prostate lobes and compared with those from 15 weeks 12T-7f tumors. One hundred micrograms protein lysate from 3 and 15 week CD-1 and 15 week 12T-7f tumor tissue were labeled with Cy2, Cy3, and Cy5 respectively, mixed and proteins separated by isoelectric point in the first dimension and molecular weight in the second dimension. The three dyes facilitated: (a) visualization of the three individual proteins under their respective wavelengths and (b) selection of protein spots differentially over- or underexpressed in the developing normal prostate (3 weeks CD-1) and prostate tumors (15 wk 12T-7f) compared to those in the 15 wk growth quiescent adult CD-1 prostate gland. Spots corresponding to these criteria were excised, treated with trypsin, and the tryptic digest analyzed by MALDI-TOF MS. The protein stathmin was identified using this approach (Fig. 1A). Stathmin expression increased 2.66-fold in the developing CD-1 prostate compared to the adult prostate. Stathmin levels were further upregulated in 12T-7f prostate tumors compared to the CD-1 developing and adult mouse prostate (2.31-fold and 5.74-fold respectively, Fig. 1B). Therefore, stathmin expression followed the anticipated pattern of a developmentally regulated protein whose expression was upregulated in tumor progression. The ion signals at $m/z = 945.51$, 1,074.58, 1,165.56, 1,312.69, 1,388.76, and 1,527.81 identified stathmin using a peptide mass mapping strategy that yielded statistically significant search scores and 36% protein coverage (Fig. 1C).

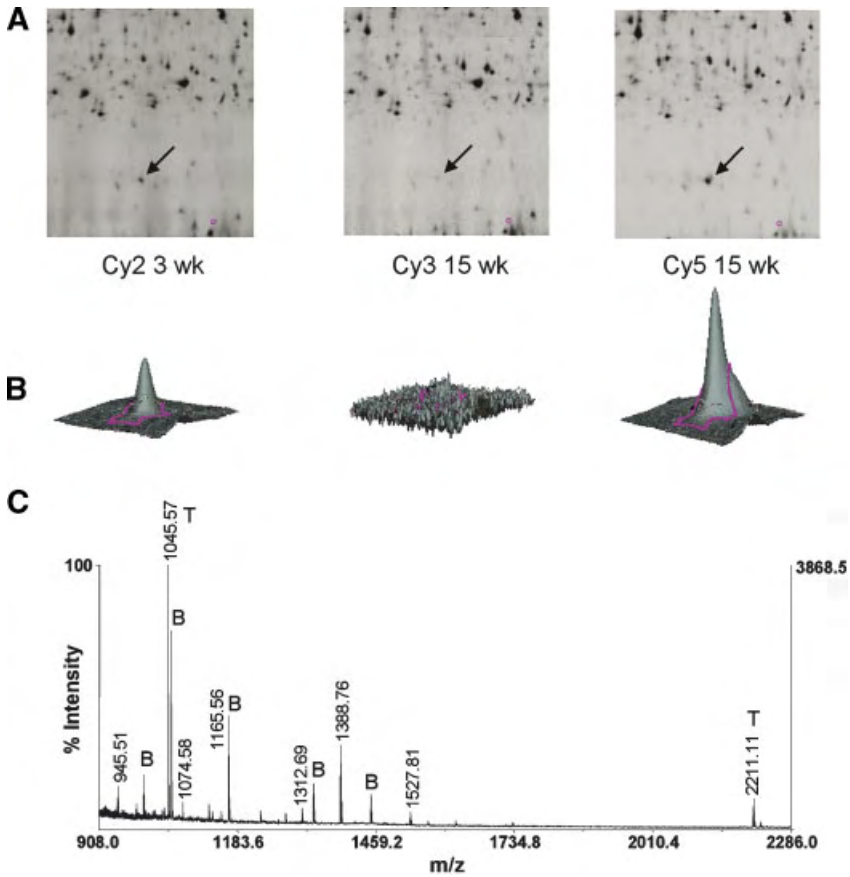

Fig. 1. Identification of Stathmin in normal prostate and prostate tumor development. **A**: Two-dimensional gel electrophoresis and Mass Spectrometry of normal mouse prostate compared to 12T-7f prostate tumors. Protein was extracted from dorsal prostate lobes representing the developing normal prostate (3 week **left panel**), the growth quiescent normal prostate (15 week, **center panel**) and the progressing tumor (15 week, **right panel**). One hundred micrograms of protein from each tissue was labeled with Cy2, Cy3, and Cy5 respectively, mixed and co-resolved by pH in the first dimension and molecular weight in the second dimension. The gel was analyzed under the respective wavelengths and spots selected that represent proteins which are upregulated in the developing normal prostate and in the 12T-7f prostate tumors. The arrow indicates the protein spot-of-interest that was determined to be stathmin. **B**: Graphical representation of stathmin protein levels. Statmin levels in the 3 weeks developing prostate increased 2.66-fold compared to the growth quiescent prostate. Stathmin expression in 15 week 12T-7f prostate tumors is elevated 2.31-fold and 5.74-fold compared to normal 3 weeks developing and 10 weeks adult prostates respectively. **C**: Protein profile of the tryptic peptides. The protein spot representing stathmin was excised, digested with trypsin as described in the Materials and Methods section and separated by MALDI-TOF MS. The tryptic peptides corresponded to stathmin.

Predicted MW and isoelectric point were consistent with the gel region.

Stathmin expression at these time points was further analyzed by IHC to identify the prostatic cell, which expresses stathmin. Tissue sections from 3- and 15-week CD-1 prostates and 15-week 12T-7f prostate tumors were stained using anti-stathmin antibody and analyzed by light microscopy. IHC analysis determined that stathmin is only expressed in luminal epithelial cells and that as expected, the highest levels of expression occur in the 3 week CD-1 prostate and in 12T-7f tumors (Fig. 2A). Western blot analysis was performed by separating 20 μg protein from these samples on 12% SDS–PAGE and probing the resulting immunoblot with anti-stathmin antibody. Again, stathmin expression was greatest in the 3-week CD-1 prostate and in 12T-7f tumors (Fig. 2B). Densitometric analysis indicated that stathmin levels in the 3-week CD-1 prostate increased 2-fold ($P < 0.05$) compared to the 15-week CD-1 prostate and that stathmin expression in 12T-7f tumors increased ~18-fold ($P < 0.05$) compared to the 15-week CD-1 prostate (Fig. 2C). These observations confirm the expression pattern of stathmin generated by two-dimensional gel electrophoresis, namely that stathmin expression is elevated in the developing prostate and that this expression is even greater in 12T-7f tumors.

We subsequently performed real-time RT-PCR to determine the levels of stathmin expression during the

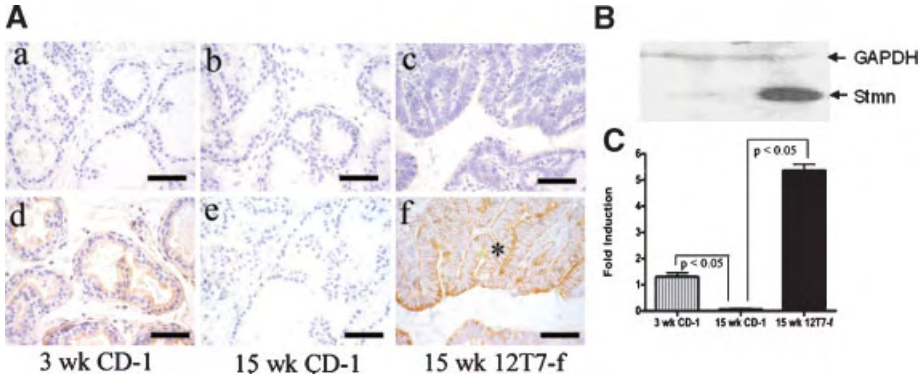

Fig. 2. Immunohistochemical (IHC) analysis of Stathmin expression in nomal prostate and 12T-7f prostate tumors. **A**: IHC Comparison of stathmin expression in CD-1 normal 3 week developing and 15 week adult prostate with 15 week 12T-7f prostate tumors. **Top Panel**: Paraffin-embedded sections were probed with HRP-conjugated anti-rabbit IgG as negative control. Scale: 50 μm. **Lower Panel**: Paraffin embedded sections were probed with rabbit anti-stathmin primary antibody and HRP-conjugated anti-rabbit IgG to detect stathmin expression. *indicates PIN lesions. Scale: 50 μm. **B**: Western Blot analysis. Protein extracts of the three tissues described in Panel A were separated by 12% SDS–PAGE, transferred to PVDF membrane and probed for stathmin expression using rabbit anti-stathmin primary antibody. **C**: Densitometric analysis of the Western blot presented in Panel B. Densitometry was performed and data was analyzed using ImageJ software. Stathmin expression was normalized to GAPDH. This graph summarizes the data of four individual Western blot analyses.

continuum for prostatic development from 2 to 5 weeks of age and in the mature prostatic gland (6 and 10 weeks of age). The numbers of prostates per time point are described in the Materials and Methods section and the time course for both CD-1 normal and 12T-7f prostate tumor samples are presented in Figure 3. In CD-1 prostates, stathmin expression was highest at 2 weeks of age and declined steadily to 5 weeks of age. This decrease correlated with completion of branching morphogenesis at 5 weeks of age. At 10 weeks of age, stathmin expression was below detection limits of the assay, suggesting that high levels of stathmin expression were not required in the growth quiescent prostate.

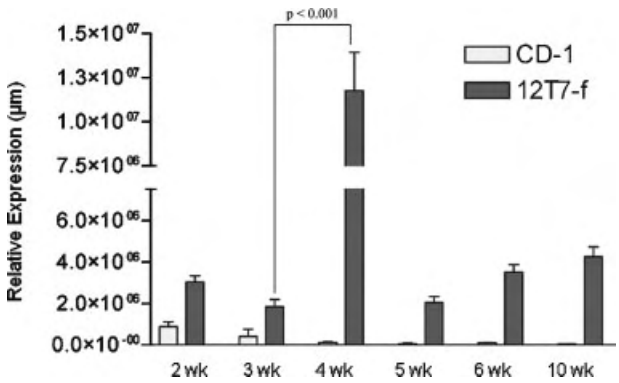

Fig. 3. Real Time RT-PCR analysis of stathmin expression in CD-1 normal and 12T-7f tumor prostates during development. RNA was extracted from 2, 3, 4, 5, 6 and 10-week-old prostates from CD-1 and 12T-7f mice and stathmin expression was quantified by Real Time RT-PCR. Number of mice per group and methodology are discussed in the Material and Methods section.

By comparison, stathmin expression in 12T-7f tumors was greater in all age groups tested. Stathmin expression decreased from 2 to 3 weeks but then unexpectedly increased sixfold compared to that in the 3 week 12T-7f prostate. This dramatic rise in stathmin expression was statistically significant ($P < 0.001$), since three sample groups consisting of 100 dorsal prostatic lobes/group were analyzed at the 4-week time point, and did not appear to correlate to known events in prostate development. At 5 weeks, stathmin levels decreased to those observed at 3 weeks after which a second rise in stathmin expression occurred and continued up to 10 weeks of age (although not to the levels seen at 4 wks). In summary, the expression pattern in normal CD-1 prostates is distinct from that in 12T-7f tumors, being highest early on in prostatic development and decreasing to nearly undetectable levels with age. In contrast, stathmin expression in 12T-7f prostates appears biphasic with a dramatic increase 4 weeks postnatally and a second lesser increase prior to the completion of prostate maturation at 5 weeks of age.

Stathmin Is Elevated During PIN and Adenocarcinoma Development in the NeoTagTissue Recombination Model

Cell lines that express stathmin in vitro and recapitulate 12T-7f tumors in vivo would be advantageous in order to analyze the mechanisms by which stathmin influences prostate growth and tumor development. In this study, we used the NeoTag1 and NeoTag2 cell lines, which were established from

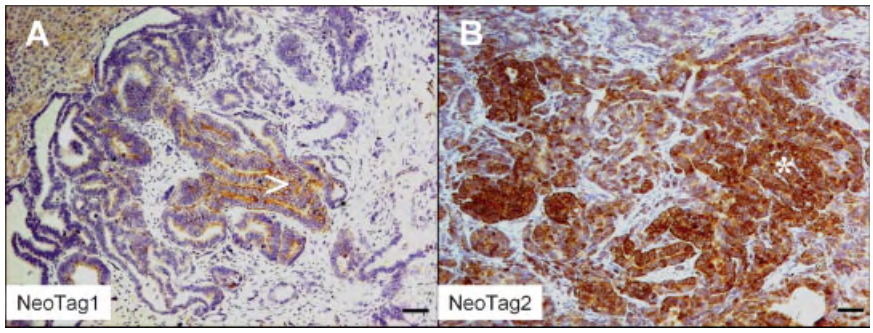

Fig. 4. Stathmin expression in NeoTag1 and NeoTag2 tumors generated by tissue recombination. NeoTag1 and NeoTag2 cells (derived from 12T-7f tumors) were recombined with rat embryonic urogenital mesenchyme and grafted under the renal capsule. This model recapitulates the original 12T-7f tumors. Paraffin-embedded sections were probed with rabbit anti-stathmin primary antibody and HRP-conjugated anti-rabbit IgG to detect stathmin expression. *, adenocarcinoma. >, prostatic intraepithelial neoplasia (PIN).

tumors obtained by crossbreeding 12T-7f mice with ARR_2PB-Neo mice to generate NeoTag bigenic mice. The establishment of the neomycin-resistant, Tag-expressing, cell lines is described in detail elsewhere [36]. Briefly, dorsolateral prostatic lobes from three 17-week-old ARR_2PBneo × LPB-Tag male mice were dissected separately and cultured, generating three individual prostate epithelial cell lines designated as NeoTag1, NeoTag2, and NeoTag3. These prostate cell lines were cultured under 10^{-8}M androgen selection and all NeoTag cell lines express the androgen receptor. In the tissue recombination assay, early passage NeoTag1 cells develop into prostate tumors, which primarily develop PIN with limited adenocarcinoma lesions whereas NeoTag2 cells develop into tumors which contain primarily adenocarcinoma with some PIN. Thus, the tissue recombinants reconstitute a phenotype that is similar to the original 12T-7f tumors in that they develop PIN. However, they also show traits consistent with tumor progression [36].

In our study, NeoTag1 cells were selected to represent PIN lesions and NeoTag2 cells were selected to represent tumor progression. IHC analyses of NeoTag1 and NeoTag2 tissue recombinants were compared to determine whether stathmin expression increased with tumor progression. As per protocol described in the Materials and Methods section, NeoTag1 and NeoTag2 tissue recombinants were established by recombining 100,000 NeoTag1/2 cells with 250,000 rat embryonic UGM cells and grafting them under the renal capsule of adult male nude mouse hosts for 4 weeks. The resulting tumors were subjected to IHC analysis to identify the cell type that expressed stathmin and to determine whether stathmin expressed increased in tumor progression from PIN to adenocarcinoma. Low levels of stathmin were observed in luminal epithelial cells of normal prostatic glands and stathmin expression increased in PIN lesions (Fig. 4 Panel A). In contrast, stathmin staining was most intense in adenocarcinoma lesions in NeoTag2 tumors (Fig. 4 Panel B), indicating that upregulation of stathmin expression coincided with PCa progression.

Increased Stathmin Expression Occurs in Human PCa

To characterize stathmin expression in human PCa, we compared archival paraffin embedded tissue sections containing PIN and adenocarcinoma adjacent to benign prostate by IHC. In benign tissue, stathmin expression was primarily localized to the basal epithelial cells of prostatic glands (Fig. 5 panels a and b). Only a few luminal epithelial cells stained positive for stathmin within any given section. In PIN lesions, stathmin expression was predictably observed in basal epithelial cells; however its expression now strongly increased in luminal epithelial cells (Fig. 5 panels c and d). Double immunofluorescence staining with anti-p63 antibody, a basal epithelial cell marker, and anti-stathmin antibody further confirmed this pattern of expression in benign cells (Fig. 5 panels f, i, and j) and PIN lesions (Fig. 5 panels h, k, and l). The prostatic stroma was always found negative for stathmin staining.

Human prostate cancer is analyzed by the Gleason grading system for diagnosis and prognosis in the treatment of men with PCa. This system defines five histological patterns with decreasing differentiation ranging from Gleason pattern 1 which identifies a well-circumscribed nodule of glands, which does not infiltrate into adjacent benign prostatic tissue to Gleason pattern 5 in which there is an almost complete loss of glandular structure and epithelial cells invade the surrounding stroma. The most prevalent plus the second most prevalent patterns are added to obtain

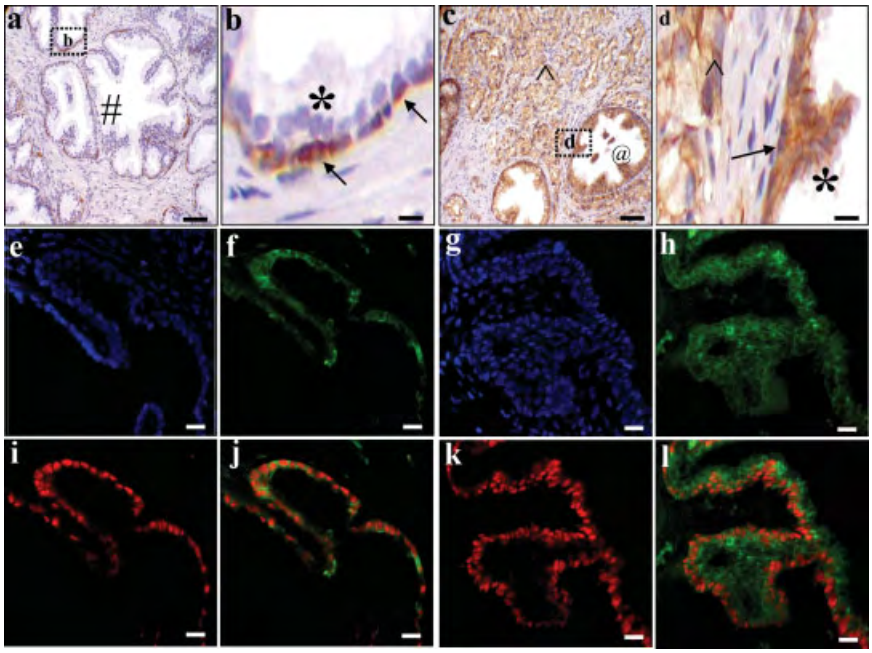

Fig. 5. Stathmin localization in benign human prostate and human prostate tumor tissue. Paraffin embedded human prostate sections containing benign, PIN and adenocarcinoma lesions were stained with anti-stathmin antibody. Panel **a**, benign human prostate tissue. Scale 50 μM. Panel **b**: Magnified region as indicated in Panel a. Scale, 10 μM. Panel **c**, PIN and adenocarcinoma. Scale 50 μM. Panel **d**, magnified region as indicated in Panel c. Scale, 10 μM. # indicates benign prostatic hyperplasia (BPH)[@]; PIN; ^ adenocarcinoma. Arrows indicate basal epithelial cells and *, luminal epithelial cells. Double fluorescence staining (Panels **e–l**) was performed to identify the cell type expressing stathmin. Archival human prostate tissue sections were stained with anti-stathmin and anti-p63 antibody. Secondary antibodies to detect stathmin and p63 were donkey anti-rabbit Alexa Fluor 488 (green) and donkey anti-mouse Alexa Fluor 594 respectively (red). Panels e (DAPI), f (stathmin), l (p63), and j (merged) represent benign prostate. Panels g (DAPI), h (stathmin), k (p63), and l (mergerd) represents PIN.

a Gleason score. We have available a prostate tissue microarray (TMA) which contains tissue cores representing BPH and Gleason patterns 3 through 5. The TMA consisted of 200 cores from a total of 50 BPH and PCa prostate biopsies (Table I). IHC analysis using anti-stathmin antibody revealed that stathmin expression significantly increased in cores containing Gleason pattern 5 compared to cores containing Gleason pattern 4 ($P < 0.05$), Gleason pattern 3 ($P < 0.01$) and BPH ($P < 0.05$) (Fig. 6). Thus, increased stathmin expression correlates with the most advanced pattern of PCa.

Stathmin Is Differentially Expressed in Androgen-Dependent and Androgen-Independent PCa Cell Lines

The observation that increased stathmin expression correlates with adenocarcinoma and local stromal invasion suggests that stathmin may play a role in tumor progression. Several cell lines that represent different aspects of advanced prostate cancer are available. These include the human PCa cell lines PC-3 and DU145 which do not require androgen for cell growth, the human LNCaP cell line which is androgen-sensitive and the mouse NeoTag1 and NeoTag2 cell lines which also require androgen for growth. These lines were tested by Western blot analysis and densitometric values were normalized to GAPDH. Stathmin levels in androgen-independent PC-3 and DU145 cells were 6-fold and 4.5 fold higher ($P < 0.05$) respectively, compared to those observed in androgen-sensitive LNCaP cells (Fig. 7, densitometric data not shown). Thus increased stathmin expression correlated with androgen-independent cell growth. Furthermore, stathmin increased 1.5-fold in NeoTag2 cells compared to NeoTag1 cells (Fig. 7), correlating with the IHC where NeoTag2 cells predominantly formed adenocarcinoma in vivo compared to NeoTag1 cells which develop primarily PIN lesions (Fig. 4).

Stathmin Is Differentially Phosphorylated in Human and Mouse Prostate Cell Lines

Stathmin contains four serines, Ser16, Ser25, Ser38, and Ser63, which are differentially phosphorylated to integrate different intracellular signals (Fig. 7a). We obtained four serine-specific phospho-antibodies to compare stathmin phosphorylation levels in the PC-3, DU145, LNCaP, NeoTag1, and NeoTag2 cell lines. Cells were cultured in their respective medium as described

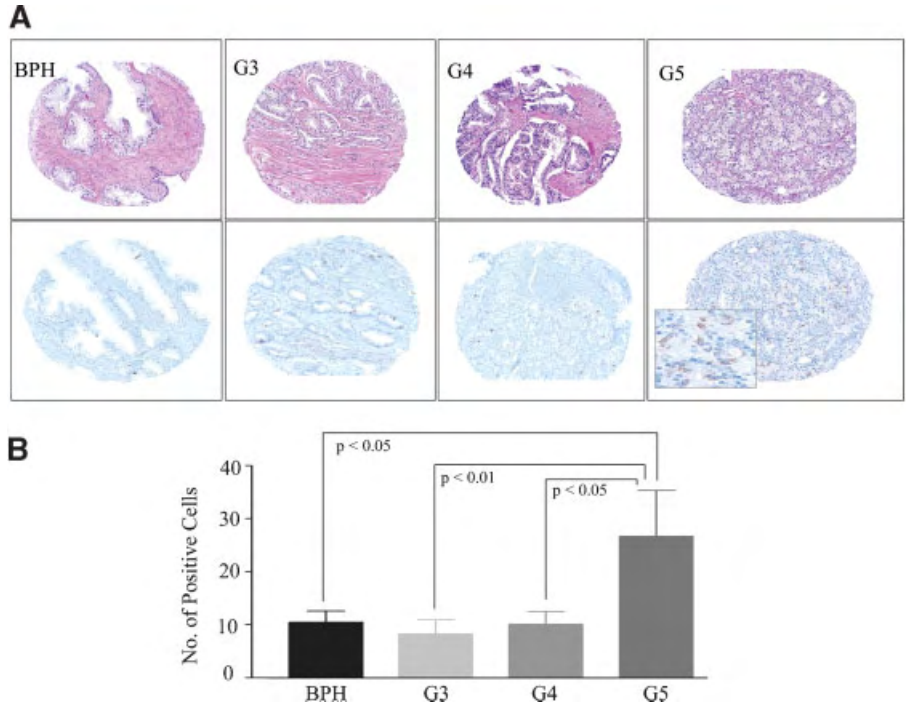

Fig. 6. Analysis of stathmin expression during human prostate cancer progression. A human prostate tissue array containing samples arranged according to increasing Gleason pattern (seeTable I) was analyzed to determine levels of stathmin expression. Panel **A**: Representative images of BPH, Gleason patterns 3, 4, and 5 human prostate specimens. Panel **B**: Stathmin expression was quantified by counting the number of stathmin positive cells per each core and the cores from each patient were averaged and graphed.

in the Methods and Materials section, harvested and subjected to Western blot analysis. As seen in Figure 7b, stathmin was phosphorylated at Ser16 in PC-3 and DU145 with the highest levels observed in PC-3 cells. Little to no phosphorylated Ser16 was detected in LNCaP cells. Conversely, phosphorylated Ser63 was greatest in LNCaP cells compared to PC-3 and DU145 cells. Hence, phosphorylation at Ser16 seems to be prevalent in androgen-independent PCa cells whereas phosphorylation at Ser63 seems to be predominant in androgen-sensitive cells. Phosphorylation at Ser25 and Ser38 were not observed in these three cell lines. This is an important observation as it may enable us to elucidate molecular pathways differentially modulated by stathmin in androgen-dependent versus androgen-independent state of the disease. In contrast, stathmin was phosphorylated at all four serines in the NeoTag1 and NeoTag2 cell lines, with phosphorylation at Ser16 being higher in NeoTag2 cells compared to that in NeoTag1 cells (Fig. 7).

Androgens and Anti-Androgens Modulate Stathmin Phosphorylation

The differential phosphorylation of Ser16 in PC-3 and DU-145 cells and Ser63 in LNCaP cells suggest that stathmin may hold divergent roles in androgen-independent compared to androgen-dependent PCa. Androgens regulate normal prostate development and they promote the development of PCa. Even during androgen deprivation therapy when androgen levels are biochemically reduced, the androgen receptor (AR) signaling pathway may still be activated through other mechanisms [37]. To elucidate which serine residues on stathmin were phosphorylated in response to androgen and anti-androgen treatment, AR-positive LNCaP cells were treated with vehicle (ETOH), DHT (10^{-8}M), hydroxyflutamide (10^{-5}M), bicalutamide (10^{-5}M), or a combination of DHT and hydroxyflutamide or DHT and bicalutamide for 24 hr. Proteins were extracted and Ser16 and Ser63 phosphorylation was analyzed by Western blot analysis.

Ser16 phosphorylation increased 2-fold with DHT treatment and 3.4-fold with hydroxyflutamide treatment (Fig. 8). The ligand binding domain of the LNCaP AR contains a threonine to alanine point mutation at amino acid 877 (T877A) which allows hydroxyflutamide to function as an agonist [38]. Thus it is possible that phosphorylation of Ser16 increased through the agonistic activity of antiandrogen treatment. In presence of both DHT and hydroxyflutamide, Ser16 phosphorylation increased nearly 9-fold in the LNCaP cells, indicating that DHT and hydroxyflutamide in combination resulted in a synergistic effect

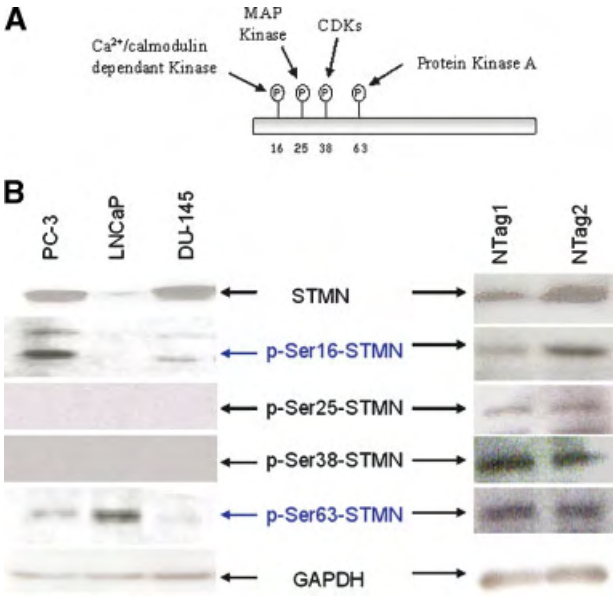

Fig. 7. Stathmin expression and phosphorylation at N-terminal Serine Residues in human and mouse prostate cell lines. Panel **A**: Diagrammatic representation of the phosphorylation sites of stathmin at Ser16, Ser25, Ser38, and Ser63. Panel **B**: Western blot analyses of stathmin expression and phosphorylation using anti-stathmin antibody and antibodies specific to the four phosphoserines of stathmin. Stathmin is conserved in rodents and humans and therefore, the phospho-antibodies recognize their respective phosphorylated serines in both species. Androgen-independent PC-3 and DU145 cells, androgen-dependent LNCaP cells, mouse NeoTag1 and NeoTag2 prostate tumor cells were cultured as described in the Materials and Methods section. Twenty micrograms of protein were loaded per lane and the pattern of stathmin phosphorylation determined.

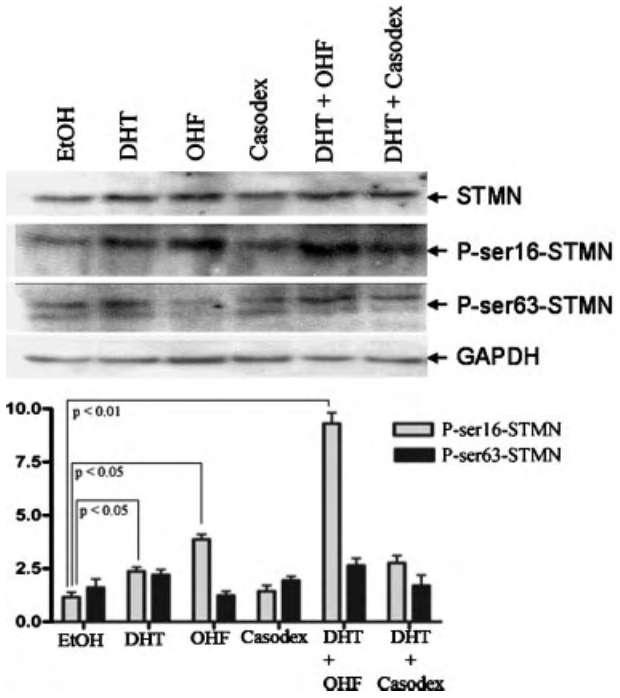

Fig. 8. Regulation of Stathmin phosphorylation by androgen and anti-androgen treatment. Panel **A**: Western blot analysis stathmin phosphorylation in response to androgen and antiandrogen treatment. LNCaP Cells were treated with 10^{-8} M dihydroxytestosterone (DHT), 10^{-8} M hydroxyflutamide (OHF), 10^{-8} M bicalutamide alone or in combination as indicated. Forty micrograms of protein were loaded per lane. Only Ser16 and Ser63 are presented since Ser 25 and Ser38 were not phosphorylated in PC-3, DU-145 or LNCaP cells. Panel **B**: Densitometric analysis of the Western blot in Panel A. Analysis was performed utilizing ImageJ software and levels of serine phosphorylation were normalized to total stathmin normalized to GAPDH. This Western blot analysis is representative of four separate experiments.

(Fig. 8). However, treatment with bicalutamide did not increase Ser16 phosphorylation over the EtOH control and did not cause a synergistic or additive effect in combination with DHT treatment. Interestingly, changes in Ser63 phosphorylation were not as pronounced as Ser16, increasing only 1.6-fold in response to DHT treatment and 1.8-fold in response to combination treatment of DHT and hydroxyflutamide treatment. The remaining treatment groups exhibited little or no induction in Ser63 phosphorylation (Fig. 8). These observations indicate that antiandrogen treatment upregulates Ser16 phosphorylation in androgen-sensitive LNCaP cells, whereas Ser16 phosphorylation in androgen-independent (PC-3 and DU145) cells is already elevated in the absence of hormonal treatment (Fig. 8).

DISCUSSION

Androgen deprivation therapy is the most used form of treatment of de novo or recurrent metastatic PCa. Unfortunately, patients with advanced metastatic disease develop androgen-independent or hormone-refractory PCa and will ultimately succumb to their disease. A number of genetic and epigenetic mechanisms have been implicated in this process including activation of AR by amplification, mutations, or growth factors, overexpression of oncoproteins, or emergence of androgen-independent cell populations (potentially from prostatic stem cells) that confer resistance to androgen deprivation therapy [37]. We discovered that stathmin expression was elevated in normal developing mouse prostates and 12T-7f tumors compared to growth quiescent adult prostates (Figs. 1–3). The pattern of this expression was similar to that of proteins such as Nkx3.1, Shh, and Notch-1, which have been implicated in the development of PCa. In PCa, Nkx3.1, and Notch-1 expression are lost (4, 5). Shh expression however, is increased in PCa (4, 5). Increased stathmin expression was also detected in human PIN and adenocarcinoma (Fig. 5). Thus, the expression pattern of stathmin parallels that of developmental factors

such as Shh and suggests that stathmin may exhibit functions similar to Shh in normal prostate development and PCa.

The ontogeny of stathmin expression during normal prostate development is significantly different from that of 12T-7f tumor development and progression. Stathmin expression is highest early during normal branching morphogenesis and declines steadily to barely detectable levels in the growth quiescent prostate (Fig. 3). Postnatally, the prostatic buds grow out through mesenchymal/epithelial interactions [39] until outgrowth ceases and the gland is fully developed at 5 weeks of age [1,2]. The increased levels of stathmin expression at 2 and 3 weeks of age imply that it may play a role during branching morphogenesis. In contrast, stathmin levels appeared elevated at all time points during tumor development. However, increase in these levels was biphasic, with an initial increase from 2 to 4 weeks and a second lesser increase, from 5 to 10 weeks of age. The mechanism for inducing the dramatic rise in stathmin levels at 4 weeks is not clear. In murine embryo fibroblast Val5 cells, induction of p53 gene resulted in a 70–90% reduction in stathmin mRNA levels [40]. Furthermore, p53 regulates stathmin expression by repressing stathmin promoter activity [41]. Thus, it is conceivable that loss of p53 activity or decreased p53 expression during development upregulate stathmin expression and thereby promote cell cycle progression. Similarly, increased stathmin expression in Gleason 5 tumors would correlate with loss of functional p53, an important but relatively late event in prostate cancer progression.

The probasin promoter is regulated by androgens and therefore probasin-driven transgene expression is upregulated early in prostatic development. In ARR_2PB-Cre mice, androgen-regulated Cre expression in prostate is detected as early as 2 weeks of age [42]. In the same way, chloramphenicol acetyl transferase (CAT) expression occurs as early as 2 weeks of age and continues to increase in parallel with sexual maturation in the LPB-CAT model [43]. In the LPB-Tag mice, expression of prostatic large T antigen (Tag) is also under control of the probasin promoter and results in the sequestration of p53 and Rb [9]. Thus, the spike in stathmin expression at 4 weeks may coincide with the loss of functional p53 through binding to the Tag protein. A p53-independent mechanism may also, in part, regulate stathmin expression since NeoTag2 cells express 1.5-fold more stathmin than NeoTag1 cells although both cell lines have similar Tag expression levels [36]. The role of stathmin during normal prostate and prostate tumor development remains to be determined.

Friedrich et al. [44] initially reported that stathmin expression increases in poorly differentiated human PCa. We performed a more extensive analysis, utilizing a tissue microarray containing tissue cores exhibiting histological changes from Gleason pattern 3 to 5, including benign tissue controls from BPH specimens. Stathmin expression is similar during Gleason patterns 3 and 4, but a significant increase in stathmin levels occurs in Gleason pattern 5 (Fig. 6), suggesting that stathmin expression parallels the development of advanced adenocarcinoma in human PCa. A similar increase is observed in NeoTag2 recombinant tumors where the development of adenocarcinoma is greater than that in NeoTag1 recombinant tumors (Fig. 4). Thus, this in vivo model could be utilized to study the mechanisms by which stathmin influences PCa progression to advanced adenocarcinoma.

Stathmin expression was also differentially localized in BPH, PIN, and adenocarcinoma. In BPH, stathmin expression occurs in the basal epithelial cell layer whereas in PIN, stathmin was present in both basal and luminal epithelial cells. In adenocarcinoma, basal cells are absent, but the epithelial cells still stain strongly for stathmin (Fig. 5). These data suggest that stathmin localization to epithelial cells and elevated expression levels represents a more advanced phenotype. Other proteins involved in PCa progression show similar patterns of expression. Matrix metalloproteinase 2 expression has been associated with tumor aggressiveness in prostate cancer. Membrane type 1-matrix metalloproteinase (MT1-MMP), an activator of latent MMP-2 (pro-MMP-2), is differentially localized to basal epithelial cells in benign prostatic glands, whereas secretory luminal epithelial cells are rarely positive. Conversely luminal epithelial cells show cytoplasmic MT1-MMP staining in HGPIN [45]. The mitogen FGF-2 is produced by stromal cells and promotes normal epithelium cell growth. However, in human PCa, epithelial cells acquire the autocrine expression of FGF-2, which may further stimulate cancer cell proliferation, enhance cell motility, and angiogenesis of primary and metastatic cancers [46]. Thus, the relocalization of stathmin to secretory epithelial cells may promote tumor aggressiveness and metastasis in PCa progression.

Several studies have indicated that stathmin promotes cell growth and tumorigenesis. Loss of stathmin expression in K562 leukemic cells abrogates anchorage independent cell growth and causes growth arrest [47]. Similarly, loss of stathmin expression in LNCaP cells have been reported to cause growth inhibition, cell cycle arrest at the G_2-M phase, increased apoptosis and decreased clonogenicity [48]. In vivo, antisense inhibition of stathmin has been shown to result in inhibition of tumorigenicity of leukemic cells [47].

Stathmin promotes microtubule destabilization by complexing with two molecules of dimeric αβ-tubulin

[49]. Phosphorylation of Ser16 and Ser63 reduces tubulin binding and inhibits stathmin-induced destabilization of microtubules in vitro [50]. Thus it is possible that in prostate cancer cells, differential Ser16 and Ser63 phosphorylation influence microtubule reorganization and differentially regulate protein kinase activity in response to androgen or antiandrogen treatment.

The anti-microtubule drug Taxotere inhibits microtubule assembly and blocks cell cycle progression similar to that seen with Taxol treatment. It has been used as chemotherapeutic agents in breast, ovarian, and PCa patients. Therefore, one strategy for the treatment of PCa would be to use anti-stathmin strategies with anti-microtubule drugs in combinatorial therapy. This may be a potent anti-cancer strategy since both therapies target the same microtubule pathway. Furthermore, stathmin antisense molecules have been reported to sensitize K562 cells to Taxol treatment, thereby inhibiting their proliferation and clonogenic potential [51]. Similar observations in breast cancer and PCa cell lines suggest that stathmin represents an important molecular target for developing novel anticancer therapies [52,53]. Combinatorial strategies that target microtubule function to inhibit the cell cycle and prevent tumor growth for treating PCa have not yet been evaluated in the clinic. Understanding the pathways, which activate stathmin expression would facilitate in designing specific combinatorial therapeutic strategies for the treatment of PCa.

Protein phosphorylation can be dysregulated in various pathological conditions and this can modulate key functions such as activity, localization, stability, and conformation. Tyrosine phosphorylation of AR in LNCaP cells by Epidermal Growth Factor (EGF) regulates AR transcriptional activity [54]. EGF-induced tyrosine phosphorylation of AR regulates nuclear localization of AR and promote AR-dependent growth of C-81 prostate cancer cells in an androgen-deprived environment [54].

Phosphorylation of serine residues modulates stathmin function. We have demonstrated the serine residues of stathmin are differentially phosphorylated, with Ser63 being primarily phosphorylated in the androgen-sensitive LNCaP cell line and Ser16 being predominantly phosphorylated in androgen-independent PC-3 and DU145 cells (Fig. 7). This differential phosphorylation suggests that the PKA signaling pathway may be more important in androgen-dependent PCa whereas PAK1/Ca^{2+}/calmodulin-dependent kinase may play a role in hormone-resistant PCa. Interestingly, Ser16 phosphorylation in LNCaP cells increased following androgen or antiandrogen treatment and treatment with DHT and antiandrogen in combination increased Ser16 phosphorylation synergistically (Fig. 8). Upregulation of Ser16 phosphorylation was also observed in androgen-independent PC-3 and DU145 in the absence of any hormonal treatment (Fig. 7), suggesting that this increase may be a mechanism by which androgen independence develops. Inhibition of stathmin phosphorylation has been reported to promote G_2/M arrest in leukemic K562 cells [30].

In summary, our study indicates that stathmin is localized to luminal secretory cells in PCa and that increased stathmin expression occurs in more advanced PCa. We also demonstrate that stathmin is differentially phosphorylated in androgen-sensitive and androgen-independent cell lines and this phosphorylation is modulated by androgen and antiandrogen treatment. It remains to be determined which pathways, alone or in combination, are activated by modulating stathmin phosphorylation status and whether this confers survival advantages on cells by promoting cell cycle progression and the development of androgen independence.

ACKNOWLEDGMENTS

Funding for this work was provided by the National Institute of Diabetes & Digestive & Kidney Diseases (R01 DK60957 and R01 DK059142) (to S.K.), the United States Department of Defense (W81XWH-06-1-0015) (to R.G.), and the Frances Williams Preston Laboratories of the T.J. Martell Foundation (to S.K.). We are grateful to Martin Gleave, M.D of The Prostate Cancer Center at the Vancouver General Hospital, University of British Columbia, British Columbia, Canada for providing the Gleason graded tissue micro-array. We are grateful to David Friedman, Ph.D. of Vanderbilt University Medical Center, Department of Biochemistry for his invaluable help in performing the two-dimensional gel-electrophoresis and mass spectrometry analysis.

REFERENCES

1. Singh J, Zhu Q, Handelsman DJ. Stereological evaluation of mouse prostate development. J Androl 1999;20:251–258.
2. Sugimara Y, Cunha GR, Donjacour AA. Morphogenesis of ductal network in the mouse prostate. Biol Reprod 1986;34:961–971.
3. Kasper S. Survey of genetically engineered mouse models for prostate cancer: Analyzing the molecular basis of prostate cancer development, progression and metastasis. J Cell Biochem 2005; 94(2) 279–297.
4. Kim MJ, Bhatia-Gaur R, Banach-Petrosky WA, Desai N, Wang Y, Hayward SW, Cunha GR, Cardiff RD, Shen MM, Abate-Shen C. Nkx3.1 mutant mice recapitulate early stages of prostate carcinogenesis. Cancer Res 2002;62(11) 2999–3004.
5. Bhatia-Gaur R, Donjacour AA, Sciavolino PJ, Kim M, Desai N, Young P, Norton CR, Gridley T, Cardiff RD, Cunha GR, Abate-Shen C, Shen MM. Roles for Nkx3.1 in prostate development and cancer. Genes Dev 1999;13(8) 966–977.

6. Wang XD, Shou J, Wong P, French DM, Gao WQ. Notch-1 expressing cells are indispensable for prostatic branching morphogenesis during development and re-growth following castration and androgen replacement. J Biol Chem 2004;279(23) 24733–24744.
7. Shou J, Ross S, Koeppen H, Sauvage FJ, Gao WQ. Dynamics of notch expression during murine prostate development and tumorigenesis. Cancer Res 2001;61(19) 7291–7297.
8. Fan L, Pepicelli CV, Dibble CC, Catbagan W, Zarycki JL, Laciak R, Gipp J, Shaw A, Lamm ML, Munoz A, Lipinski R, Thrasher JB, Bushman W. Endocrinology. 2004;145(8) 3961–3970.
9. Kasper S, Sheppard P, Yan Y, Pettigrew N, Borowsky AD, Prins G, Dodd JG, Duckworth ML, Matusik RJ. Development, progression and androgen dependence of prostate tumors in probasin-large T antigen transgenic mice: A model for prostate cancer. Lab Invest 1998;78(6) i–xv.
10. Kasper S, Tu W, Roberts RL, Shappell SB. Transgenic mouse models for prostate cancer. Identification of an androgen-dependent promoter and creation and characterization of the long probasin promoter- Large T antigen (LPB-Tag) model. Methods Mol Med 2003;81:113–147.
11. Kasper S, Smith JA. Genetically modified mice and their use in developing therapeutic strategies for prostate cancer. J Urol 2004;172:12–19.
12. Pasmantier R, Danoff A, Fleischer N, Schubert UK. p19, a hormonally regulated phosphoprotein of peptide hormone producing cells; secretagogue-induced phosphorylation in AtT-20 mouse pituitary tumor cells and in rat and hamster insulinoma cells. Endocrinology 1986;119:1229–1298.
13. Cooper HL, McDuffe E, Braverman R. Human peripheral lymphocyte growth regulation and response to phorbol esters is linked to synthesis and phosphorylation of the cytosolic protein, prosolin. J Immunol 1989;143:956–963.
14. Ferrari AC, Seuanez HN, Hannah SM, Atweh GF. A gene that encodes for a leukemia associated phosphoprotein (p18) maps to chromosome bands 1p35-36.1. Genes Chromosome Cancer 1990; 2:125–129.
15. Schubert UK, Xu J, Fan W, Cheng G, Goldstein H, Alpini G, Shafrritz DA, Amat JA, Farooq M, Norton WT, Owen TA, Lian JB, Stein GS. Widespread and differentiation stage specific expression of the gene encoding phosphoprotein p19 (Metablastin) in mammalian cells. Differentiation 1992;51:21–32.
16. Brattsand G, Roos G, Marklan U, Ueda H, Landberg G, Nanberg E, Sideras P, Gulber M. Quantitative analysis of the expression and regulation of an activation-regulated phosphoprotein (oncoprotein 18) in normal and neoplastic cells. Leukemia 1993;7:569–579.
17. Nylander K, Markund U, Brattsand G, Gullberg M, Roos G. Immunohistochemical detection of oncoprotein 18 (Op18) in malignant lymphoma. Histochem J 1995;27(2) 155–160.
18. Rowlands DC, Williams A, Guest J, Reynolds GM, Barber PC, Brown G. Stathmin expression is a feature of proliferating cells of most, if not all, cell lineages. Lab Invest 1995;72(1) 100–113.
19. Ahn J, Murphy M, Kratowicz S, Wang A, Levine A, George D. Downregulation of stathmin/Op18 and FKB25 genes following p53 induction. Oncogene 1999;18:5954–5958.
20. Budde P, Kumagai A, Dunphy W, Heald R. Regulation of Op18 during spindle assembly in Xenopus egg extracts. J Cell Biol 2001;153:149–157.
21. Curmi PA, Nogues C, Lachkar S, Carelle N, Gonthier MP, Sobel A, Lidereau R, Bieche I. Overexpression of stathmin in breast carcinomas point out to highly proliferative tumors. British J Cancer 2000;82:142–150.
22. Price DK, Ball Jr, Bahrani-Mostafavi Z, Vachris JC, Kaufman JS, Naumann Rw, Higgins RV, Hall JB. The phosphoprotein Op18/stathmin is differentially expressed in ovarian cancer. Cancer Invest 2000;18:722–730.
23. Luo X, Mookerjee A, Ferrari A, Mistry S, Atweh GF. Regulation of phosphoprotein p18 in leukemic cells: Cell cycle regulated phosphorylation by p34-cdc2 kinase. J Biol Chem 1994;269: 10312–10318.
24. Mistry S, Atweh G. Role of stathmin in the regulation of mitotic spindle: Potential applications in cancer therapy. Mount Sinai J Med 2002;69(5) 299–304.
25. Sobel A, Boutterin MS, Beretta L, Chneiweiss H, Doye V. Intracellular substrates for extracellular signaling. Characterization of a ubiquitous neuron enriched phosphoprotein (stathmin). J Biol Chem 1989;264(7) 3765–3772.
26. Horwitz SB, Shen HJ, He L, Dittmar P, Neef R, Chen J, Schubert UK. The microtubule destabilizing activity of metablastin (p19) is controlled by phosphorylation. J Biol Chem 1997;272:8129–8132.
27. Gavet O, Ozon S, Manceau V, Lawler S, Curmi P, Sobel A. The stathmin phosphoprotein family: Localization and effects on the microtubule network. J Cell Sci 1998;111:3333–3346.
28. Wittmann T, Bokoch GM, Waterman-Storer CM. Regulation of microtubule destabilizing activity of Op18/stathmin downstream of Rac1. J Biol Chem 2004;279(7) 6196–6203.
29. Monet C, Gavard J, Mege RM, Sobel A. Clustering of cellular prion protein induces ERK1/2 and stathmin phosphorylation in GT 1-7neuronal cells. FEBS Lett 2004;576:114–118.
30. Marklund U, Brattasand G, Shingler V, Gulberg M. Serine 25 of Oncoprotein 18 is a major cytosolic target for the mitogen activated protein kinase. J Biol Chem 1993;268(20) 15039–15049.
31. Marklund U, Brattasand G, Osterman O, Ohlsson P, Gullberg M. Multiple signal transduction pathways induce phosphorylation of serines 16,25 and 38 in T Lymphocytes. J Biol Chem 1993; 268(34) 25671–25680.
32. Marklund U, Osterman O, Melander H, Bergh A, Gullberg M. The phenotype of a ''Cdc2 kinase target site-deficient'' mutant of oncoprotein 18 reveals a role of this protein in cell cycle control. J Biol Chem 1994;269:30626–30635.
33. Curmi PA, Maucuer A, Asselin S, Lecourtois M, Chaffotte A, Schmitter JM, Sobel A. Molecular characterization of human stathmin expressed in Escherichia coli: Site-directed mutagenesis of two phosphorylatable serines (Ser-25 and Ser-63). Biochem J 1994;300(Pt 2):331–338.
34. Küntziger T, Gavet O, Sobel A, Bornens M. Differential Effect of Two Stathmin/Op18 Phosphorylation Mutants on *Xenopus* J Cell Biol 2001;276:22979–22984.
35. Gradin HM, Larsson N, Marklund U, Gullberg M. Regulation of microtubule dynamics by extracellular signals: cAMP-dependent protein kinase switches off the activity of oncoprotein 18 in intact cells. J Cell Biol 1998;140:131–141.
36. Wang W, Kasper S, Yuan J, Jin RJ, Zhang J, Ishii K, Wills M, Hayward S, Matusik RJ. Androgen-dependent prostate epithelial cell selection by targeting ARR2PBneo to the LPB-Tag model of prostate cancer. Lab Invest 2006;86:1074–1088.
37. Feldman BJ, Feldman D. The development of androgen-independent prostate cancer. Nature Rev Cancer 2001;1(1) 34–45.
38. Veldscholte J, Ris-Stalpers C, Kuiper GG, Jenster G, Berrevoets C, Claassen E, van Rooij HC, Trapman J, Brinkmann A, Mulder E. A

mutation in the ligand binding domain of the androgen receptor of human INCaP cells affects steroid binding characteristics and response to antiandrogens. Biochem Biophys Res Commun 1990;173(2) 534–540.

39. Chang WY, Wilson MJ, Birch L, Prins GS. Neonatal estrogen stimulates proliferation of periductal fibroblasts and alters the extracellular matrix composition in the rat prostate. Endocrinology 1999;140(1) 405–415.
40. Ahn J, Murphy M, Kratowicz S, Wang A, Levine A, George D. Down-regulation of the stathmin/Op18 and FKBP25 genes following p53 induction. Oncogene 1999;18:5954–5958.
41. Johnsen JI, Aurelio ON, Kwaja Z, Jorgensen GE, Pellegata NS, Plattner R, Stanbridge EJ, Cajot J. P-53 mediated negative regulation of stathmin/Op18 expression is associated with G_2/M cell-cycle arrest. Int J Cancer 2000;88:685–691.
42. Wu X, Wu J, Huang J, Powell W, Zhang J, Matusik R, Sangiorgi F, Maxson R, Sucov H, Roy-Burman P. Generation of a prostate epithelial cell-specific Cre transgenic mouse model for tissue-specific gene ablation. Mechan Dev 2001;101:61–69.
43. Yan Y, Shephard PC, Kasper S, Lin L, Hoare S, Kapoor A, Dodd JG, Duckworth ML, Matusik RJ. Large fragment of the probasin promoter targets high levels of transgene expression to the prostate of transgenic mice. Prostate 1997;32(2) 129–139.
44. Friedrich B, Gronberg H, Landstorm M, Gullber M, Bergh A. Differentiation-stage specific expression of oncoprotein 18 in human and rat prostatic adenocarcinoma. Prostate 1995;27(2) 102–109.
45. Upadhyay J, Shekarriz B, Nemeth JA, Dong Z, Cummings GD, Fridman R, Sakr W, Grignon DJ, Cher ML. Membrane type 1-matrix metalloproteinase (MT1-MMP) and MMP-2 immunolocalization in human prostate: Change in cellular localization associated with high-grade prostatic intraepithelial neoplasia. Clin Cancer Res 1999;5:4105–4110.
46. Djakiew D. Dysregulated expression of growth factors and their receptors in the development of prostate cancer. Prostate 2000; 42:150–160.
47. Jeha S, Luo XN, Beran M, Kantarjian H, Atweh GF. Antisence RNA inhibition of phosphoprotein p18 expression abrogates the transformed phenotype of leukemic cells. Cancer Res 1996;56(6) 1445–1450.
48. Mistry SJ, Bank A, Atweh GF. Targeting stathmin in prostate cancer. Mol Cancer Therap 2005;4(12) 1821–1829.
49. Jourdain L, Curmi P, Sobel A, Pantaloni D, Carlier MF. Stathmin: A tubulin-sequestering protein which forms a ternary T2S complex with two tubulin molecules. Biochemistry 1997;36: 10817–10821.
50. Paolo GD, Antonsson B, Kassel D, Riederer BM, Grenningloh G. Phosphorylation regulates the microtubule-destabilizing activity of stathmin and its interaction with tubulin. FEBS Lett 1997;416:149–152.
51. Iancu C, Mistry S, Arkin A, Atweh GF. Taxol and anti-stathmin therapy: A synergistic combination that targets the mitotic spindle. Cancer Res 2000;60:3537–3541.
52. Ali E, Bash-Babula J, Yang J, Hait W. Effects of stathmin on the sensitivity to antimicrotubule drugs in human breast cancer. Cancer Res 2002;62:6864–6869.
53. Mistry SJ, Atweh GF. Therapeutic interaction between stathmin inhibition and chemotherapeutic agents in prostate cancer. Mol Cancer Therap 2006;5:3248–3257.
54. Guo Z, Dai B, Jiang T, Xu K, Xie Y, Kim O, Nesheiwat I, Kong X, Melamed J, Handratta VD, Njar VCO, Brodie A, Yu L, Veenstra TD, Chen H, Qiu Y. Regulation of androgen receptor activity by tyrosine phosphorylation. Cancer Cell 2006;10:309–319.